DESERT PAVEMENT MORPHOLOGY AND DYNAMICS,

BIG BEND NATIONAL PARK, TEXAS

A Thesis

by

COURTNEY MICHELLE HARMON

Submitted to the Office of Graduate Studies of
Texas A&M University
in partial fulfillment of the requirements for the degree of

MASTER OF SCIENCE

December 2006

Major Subject: Geography

DESERT PAVEMENT MORPHOLOGY AND DYNAMICS,

BIG BEND NATIONAL PARK, TEXAS

A Thesis

by

COURTNEY MICHELLE HARMON

Submitted to the Office of Graduate Studies of
Texas A&M University
in partial fulfillment of the requirements for the degree of

MASTER OF SCIENCE

Approved by:

Chair of Committee,	Vatche P. Tchakerian
Committee Members,	Michael R. Waters
	Andrew Hajash, Jr.
Head of Department,	Douglas J. Sherman

December 2006

Major Subject: Geography

ABSTRACT

Desert Pavement Morphology and Dynamics,

Big Bend National Park, Texas. (December 2006)

Courtney Michelle Harmon, B.S., Texas A&M University

Chair of Advisory Committee: Dr. Vatche P. Tchakerian

Desert pavements consist of a one- to two-layer thick surface armory of stones overlying finer, virtually stone-free material which often adopts the appearance of a meticulously tiled mosaic. They cover half of the arid land surface in North America and are usually concentrated on low-sloping alluvial fans and desert piedmont surfaces. McFadden et al. (1987) suggested the accretionary mantle model of desert pavement formation, following research on pavements atop the Cima volcanic complex in the Mojave Desert. However, the wide-spread applicability of this model to diverse lithologies and geomorphic environments remains to be seen. No research has been conducted on desert pavement at Big Bend National Park (BBNP), Texas, despite the occurrence of well-developed pavements in the park and surrounding regions of the Chihuahuan Desert. This research highlights three diverse desert pavement sites at BBNP through a detailed geomorphic assessment including location of desert pavement distribution, classification into surface mosaic units, examination of sediment and soil characteristics, and determination of lithology of the pavement clasts.

At each BBNP study area, values for desert pavement clast size, sorting, and percent ground cover were compared to the parameters set forth in Wood et al. (2002) to

classify the desert pavements into surface mosaics based on degree of development. Sediment analysis and soil profile photographs were used to characterize the surface sediments and subsurface soil horizons. To determine geologic origin, dominant lithologies of the pavement clasts were compared to outcrop and bedrock samples and to published geologic maps of BBNP.

Desert pavements in this study differ significantly in surface texture, soil characteristics, geologic origin, and degree of development compared to the typical pavements of the Mojave Desert used in much of the fundamental research. Results indicate that the desert pavements at BBNP may not have been derived from bedrock and evolved *in-situ*, as suggested by the accretionary mantle model. Primarily, a combination of fluvial processes and weathering appears more influential to desert pavements in the semi-arid environment of BBNP. This study presents a new perspective on desert pavement geomorphology in Big Bend National Park and serves as a baseline for continued research.

ACKNOWLEDGEMENTS

I extend great appreciation to:

Dr. Tchakerian for sparking my interest in this research and for being a constant source of advice, guidance, and knowledge;

Dr. Hajash and Dr. Waters for their input and service on my committee;

The Department of Geography for encouraging my conference presentations, professional development, and international excursions;

The National Park Service, Big Bend National Park, George Bush Presidential Library Foundation, and the Texas A&M Soil Characterization Lab for funding and supporting my field research;

Joni and Kirk for patiently teaching me GIS;

Paul for fun and fieldwork in Big Bend;

Jean for braving freezing temperatures and hungry javelina, and for being a tremendous friend;

And finally, my Geography graduate student colleagues for camaraderie and countless memories along the way.

TABLE OF CONTENTS

Page

LIST OF FIGURES

FIGURE Page

LIST OF TABLES

INTRODUCTION

1.1 Section Introduction

Desert pavements (a type of stone pavement) consist of a one- to two-layer thick surface of armory stones overlying finer, virtually stone-free material which often appears as a meticulously tiled mosaic (Fig. 1). They cover more than half of the arid land surface in North America (Evenari, 1985), and are usually concentrated on low-sloping alluvial fans and desert piedmont surfaces. Desert pavement plays a key role in many arid land ecosystem processes including vegetation distribution, topography, hydrology, and pedology (Cooke et al., 1993). Their vast distribution and noted geomorphic influence in drylands justify desert pavements as a topic of particular importance in desert research.

Most of the major studies on desert pavement geomorphology during the past twenty years have taken place in the Mojave Desert of California (Wells et al., 1985; McFadden et al., 1987; Anderson et al., 1994; Wood et al., 2002; 2005). Numerous explanations have been offered for desert pavement formation including deflation, fluvial processes, upward migration of stones, and concentration by weathering (Cooke et al., 1993). Current literature favors the accretionary mantle model of desert pavement formation, developed on basaltic rocks in the Cima volcanic field of the eastern Mojave Desert in California (McFadden et al., 1987). However, the wide-spread applicability of this model to diverse lithologies and geomorphic environments remains to be fully seen.

This thesis follows the style of Journal of Arid Environments.

Fig. 1. Landscape and close-up views of desert pavement, BBNP, Texas.

No major geomorphic studies on desert pavements have been conducted in the Chihuahuan Desert of North America.

The Chihuahuan Desert is the largest desert in North America (518,000 km^2) with one-fourth located in western Texas and the remainder in northern Mexico (Laity, 2002). Big Bend National Park (BBNP) shown in Fig. 2 includes the largest protected area of the Chihuahuan Desert in the United States, over 3,000 km^2 (National Park Service, 2006). Furthermore, the National Park Service (2006) has deemed BBNP one of the least researched (and visited) of all the national parks in the United States. A thorough literature review and consultation with park scientists reveals that no studies have been conducted on desert pavement at BBNP, Texas, despite the occurrence of well-developed pavements in the park and in the adjacent regions of the Chihuahuan Desert.

1.2 Purpose Statement

The purpose of this thesis is to describe the morphology and dynamics of the desert pavements in BBNP. Also, this study will evaluate the various hypotheses of desert pavement formation in yet another geographic and geomorphic setting. This study also serves as a baseline for continued studies on local desert pavement distribution, anthropogenic disturbance and recovery, effect on geomorphic processes, and large-scale surficial mapping projects at BBNP.

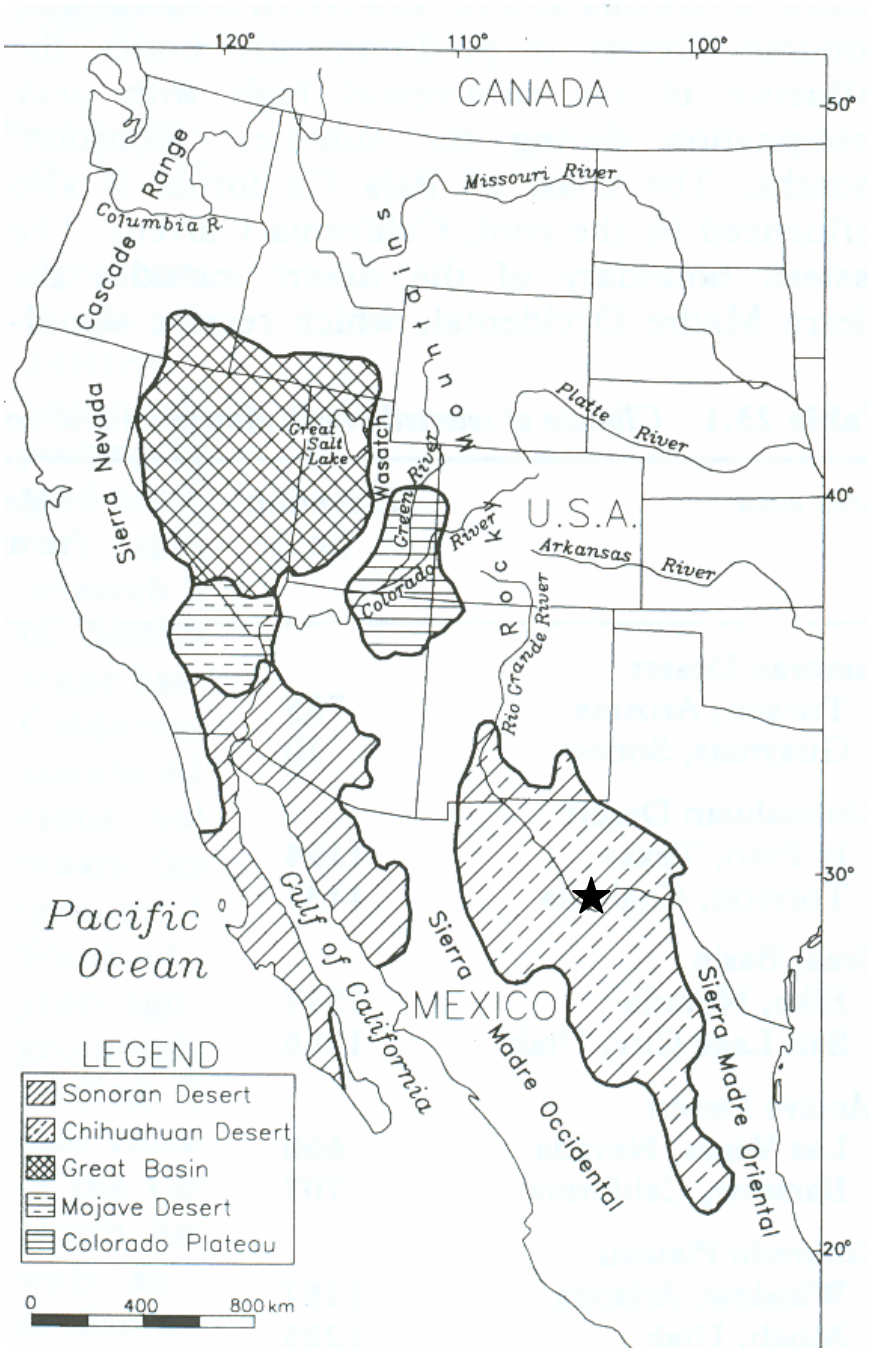

Fig. 2. Location of Big Bend National Park. The star marks the center of BBNP, which encompasses more than 3,000 km^2 of the Chihuahuan Desert in western Texas, USA. (Modified from Tchakerian, 1997).

1.3 Objectives

The primary objectives of this study are to:

1) locate, describe, and classify the morphology of desert pavement fields. Detailed textural description and surficial mapping will comprise the initial steps toward understanding many aspects of desert pavement including its development, hydrologic response, and role in the larger ecosystem (Higgitt and Allison, 1999; Wood et al., 2002);

2) determine the lithology of the desert pavement clasts. Correlating the dominant geologic composition of the pavement clasts with local lithology will establish the source rock from which the pavement was likely derived;

3) describe the sediments and the subsurface soil horizons that lie immediately beneath the desert pavement; and

4) evaluate the applicability of the accretionary mantle model of desert pavement formation, developed in the Mojave Desert, to those of the Chihuahuan Desert at BBNP.

BACKGROUND

2.1 General Description of Desert Pavements

Desert pavements (stone pavements) consist of a one- to two-layer thick surface of armory stones, ranging in size from boulders to fine gravels, overlying finer, virtually stone-free material (Mabbutt, 1977). They are common in sparsely vegetated areas of arid lands atop mantles of weathered debris, alluvial fans, and topographically level soil surfaces on desert piedmonts, and have a millennial time scale of formation. On a well-developed stone pavement, the clasts can touch and even overlap neighboring clasts to form the appearance of a meticulously tiled mosaic, and the individual stones are sometimes covered in rock varnish (Cooke and Warren, 1973). Without identifying desert pavement by name, Hume (1925, p 62) described the Egyptian Desert as "a plain of bare rock fragments shimmering in the sunlight."

Stone pavements in the southwestern United States are commonly referred to as *desert pavements*, a term specific to North America which is used to describe very smooth, flat, pebble-sized pavements that develop on the lower sections of alluvial fan surfaces. This study will use the term desert pavement. Like many other geomorphic features, stone pavements have taken on several local names throughout the world, such as *stony mantles* or *gibber plains* in Australia, *hammada* or *reg* in North Africa and the Middle East, and *gobis* in central Asia (Mabbutt, 1977; Tchakerian, 1999b).

2.2 Geomorphology

Desert pavements play an integral role in many arid land ecosystem processes. The coarse layer of stones that mantles the surface is an erosional barrier that promotes surface stability much like vegetation does, and protects the desert soil horizons below. Desert pavements act as a storage area for aeolian sediments (both dust and sand) in transit, and also impact desert surface overland flow and infiltration by increasing runoff and decreasing infiltration in areas of well-developed desert pavements. Because desert pavements recover slowly after being disturbed, they preserve a long record of the processes that have been acting upon the surface. They are particularly susceptible to destruction by human impact and off-road vehicles which remove the protective armoring, leaving the newly exposed soil susceptible to accelerated wind and water erosion (Cooke et al., 1993; Tchakerian, 1999b).

Al-Farraj and Harvey (2000) used morphological differences in desert pavement to correlate terraces and alluvial fans in Oman and U.A.E. and to estimate their relative ages. Using a simple index of desert pavement development – including clast fracturing and angularity, size, sorting, packing, and surface texture – the limestone clasts of these desert pavements were classified. The authors found that the weakly-developed pavements were located atop the youngest terrace and fan surfaces, while the well-developed pavements corresponded to the highest terraces and oldest fan surfaces.

Haff (2001) suggests that desert pavement holds an even more important role as an indicator of subtle environmental changes, which he refers to as an ‘environmental canary.’ Pavement stones are often only loosely cemented to the underlying matrix or to

each other, and a simple footstep can dislodge them. The longevity of these surfaces is dependent upon a stable local environment away from disruptive anthropogenic forces. Therefore, an abundance of newly overturned varnished pavement clasts, as observed by Haff in Death Valley National Park, may provide evidence for recent environmental changes in deserts. Haff (2001) concludes that the high number of overturned stones in Death Valley National Park is rare on the millennial time scale of desert pavement formation, and this phenomena is largely the result of increased animal traffic and foraging and heightened bioturbation of vegetation in response to recent intense El Niño precipitation. Studying the response of desert pavements to climatic and biologic perturbations could shed light on the role of desert pavement surfaces as indicators of broader environmental change.

Rock coatings cover many bare rock desert surfaces, and their presence infers long-term stability (Watson and Nash, 1997). The three most common coatings are rock varnish, silica glaze, and iron films. Rock varnish is a thin (less than 100 μm) chemical deposit containing clay minerals, manganese, and iron oxide that darkens the surface of some desert rocks (Dorn, 2004). Although controversial, rock varnish has been used for relative and absolute dating of desert surfaces.

2.3 Disturbance and Recovery

Although desert pavements are often regarded as stable geomorphic landforms, their surfaces have dynamic, not static, stability, punctuated by periods of disturbance and recovery (Haff and Werner, 1996). Numerous studies have investigated the impacts

of military maneuvers on desert pavement surfaces, most notably by Belnap and Warren (2002), El-Baz (1992), and Kade and Warren (2002). El-Baz (1992) concluded that desert pavement disruption in Kuwait, as a result of Gulf War I military maneuvers, exposed the desert soil beneath pavements to wind and soil erosion for many centuries to come.

Additionally, a study by Belnap and Warren (2002) showed that, 55 years after desert pavement disturbance by General George S. Patton's military vehicles during training operations, the impact was still visible especially in areas of mature pavements in the Mojave Desert. Kade and Warren (2002) also point out that tent-city construction and the foot traffic on military training base camps had also destroyed pavements in the Sonoran Desert, leaving scars long after the military camp was abandoned in 1944.

Haff and Werner (1996) attempted to quantify the response of desert pavement to a disturbance. In a five-year field experiment in Panamint Valley, California, clasts were removed from the desert pavement surface in square plots to reveal the soil layer below in an effort to study the processes and rate of desert pavement recovery. In studying the resurfacing process, Haff and Werner found that gaps caused by the removal of tiny stones had completely healed in five years. The authors, therefore, concluded that the larger the disturbance area of desert pavement, the slower the rate at which it will recover. The recovery rate of desert pavements is, however, a function of several factors including the availability of stones, the magnitude and variety of mobilizing forces, and the microtopography of the surface.

In general, the stones which mobilized to infill the disturbed area were smaller than the clasts that made up the original pavement surface, and stones of greater than 1cm remained in the same location over the five-year period. First-hand observations of clast motions are often spotty and unrepresentative, and there was no evidence of any clast-moving forces to a degree significant enough to mobilize the clasts needed to infill the cleared plots. Therefore, the authors did not offer an exact recovery process for this study site, but concluded that small stones appear to be re-emplaced from one dominant direction, indicating that a uni-directional process must be responsible for the recovery.

2.4 Desert Pavement Formation

The precise mechanism for desert pavement formation remains a controversial topic, as several hypotheses exist regarding their formation. These include: a) the deflation of fine sediments by wind, b) the removal of fines by fluvial action, c) the upward migration of stones, d) concentration by subsurface weathering, and e) surface-derived desert pavement clasts rising vertically on an accreting mantle of soil (Cooke, 1970; Mabbutt, 1977; McFadden et al., 1987; Tchakerian, 1999b). In all cases, the formation and preservation of desert pavement is contingent on the abandonment of the surface when it becomes isolated from the surrounding area by incision or diversion of overland flow elsewhere.

2.4.1 Deflation

The deflation hypothesis suggests that a heterogeneous mixture of clay- to cobble-sized sediments is acted upon by the wind, the latter removing the fine sand and dust particles. The coarse materials are left behind and concentrate to form a lag deposit that mantles the surface of the desert floor (Cooke and Warren, 1973). Deflation alone, however, cannot account for the existence of many desert pavements with subsurface soil layers and the virtually stone-free underlying materials (Cooke et al., 1993).

2.4.2 Fluvial Action

Still other literature suggests that water is the dominant force in desert pavement formation (Lowdermilk and Sudling, 1950). This occurs either by surface runoff washing finer textured soils off desert slopes, or by high-intensity desert precipitation events which produce raindrops that impact and dislodge the finer sediments on the surface. Similar to deflation, fine sediments are removed by water, leaving behind the coarse stones to form a desert pavement. Sharon (1962) demonstrated the importance of surface runoff at pavement sites in Israel, and Cooke et al. (1993) noted fluvial erosion at various sites throughout California.

2.4.3 Upward Migration

The concentration of coarse clasts at the surface and the distinct lack of similarly sized particles below lead to the hypothesis that the stones originated below the surface and migrated upward (Springer, 1958). Jessup (1960) observed the migration of coarse

particles following twenty-two repeated wet/dry cycles in laboratory experiments. This hypothesis is undermined, however, by the fact that few stones are actually observed in transition upward in field experiments.

2.4.4 Concentration by Subsurface Weathering

Stones embedded in moist soil are more susceptible to weathering (mechanical, chemical, and biological weathering) than stones at the surface, therefore surface pavement clasts may survive above soils containing little stone (Mabbutt, 1977). Fan terraces in eastern Sinai Desert, Egypt exhibit this phenomenon, as granitic desert pavement clasts concentrate atop grus formed by simultaneous weathering of granite boulders below the surface. This process is more common in moist desert environments, since water accelerates weathering processes.

2.4.5 Accretionary Mantle Model

Based on work in central Australia, Mabbutt (1977) suggested that desert pavements result from processes of cumulic pedogenesis, upward sorting of clasts through a fine textured soil mantle. McFadden et al. (1987), working on desert pavements atop the Cima volcanic complex (a 560,000 year old basalt field in the eastern Mojave Desert, California), were the first to provide field-based evidence that desert pavements are created at the land surface and remain there through aeolian deposition and concurrent development of soils underneath the pavement (Fig. 3). Similarly to Mabbutt (1977), McFadden et al. proposed that the deposited pavement

Fig. 3. Desert pavement at Cima Volcanic Field, Mojave Desert.
(Top) Soil pit beneath desert pavement exposing vesicular horizon and aeolian mantle.
(Bottom) Landscape view of basaltic desert pavement.
Photos taken in 1998 by V.P. Tchakerian.

clasts rise upward on a vertically accreting soil mantle through a process termed the accretionary mantle model, as shown in Fig. 4.

McFadden et al. (1987) suggested the seminal processes for pavement formation and surface evolution. First, clasts are derived *in situ* from basaltic bedrock from topographically high areas that are mechanically weathered. This weathering process leads to the formation of a rubble layer that fills in topographically low areas, thus smoothing out the surface and creating a layer of armored stones atop the parent bedrock. Second, soil is concurrently developed beneath the pavement, causing the clasts to rise vertically (Anderson et al., 1994). Windblown dust from nearby playas and dunes accumulates on the desert floor and becomes incorporated into the subsurface vesicular soil horizon, which is rich in aeolian silt and clay and has a columnar structure (Wells, et al., 1998). The seasonal changes of this soil layer, particularly the upward doming of ped tops and vertical displacement of the overlying clasts in the summer, and their subsequent collapse during the winter, constantly maintains the pavement clasts on the surface while soil layers develop and thicken underneath.

Wells et al. (1995) supported this model by comparing *in-situ* cosmogenic ^{3}He exposure ages of pavement clasts to the bedrock source exposure age. Their results showed similarity in age between un-eroded bedrock and pavement beginning to form nearby, and age correlation between several desert pavement fields and their underlying basalt flows. This field evidence from the Cima Volcanic Field supports the born-at-the-surface desert pavements depicted in the accretionary mantle model.

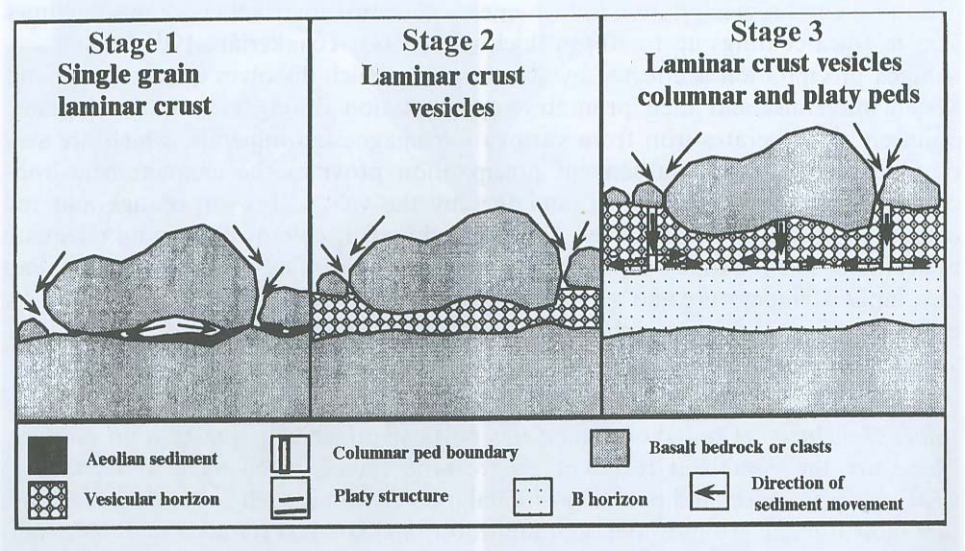

Fig. 4. Accretionary mantle model of desert pavement formation as first proposed by McFadden et al. (1987). Image from Tchakerian (1999a).

It is very likely that a combination of the above processes is required for desert pavement formation. In particular, Dixon (1994) notes that clast source is central to the understanding of desert pavement development, and that there are two principal sources: clasts disintegrated from bedrock and fluvially deposited clasts. Recently, Williams and Zimbelman (1994) made the case for sheetflood being the primary process for the emplacement of pavement clasts, since a young, well-developed desert pavement was observed immediately overlying bare rock on the Pisgah basalt flow in the Mojave Desert, California. The authors suggest that the deposition by sheetflow could represent an initial substage of the accretionary model where overland flow of water was responsible for the initial creation of the desert pavement, and a vesicular soil horizon subsequently formed beneath it, rather than the pavement and soil horizon coevolving.

2.5 Desert Pavement Classification

A desert pavement classification system was developed by Wood et al. (2002) on the Cima volcanic field in the eastern Mojave Desert, California based on such textural parameters as percent ground cover, clast size, and sorting. Three distinct surface mosaic types of bare ground (BG1, BG2, BG3) and three desert pavement mosaic types (DP1, DP2, DP3) were identified as shown in Fig. 5, and each desert pavement mosaic was determined to be “unique, precise, and consistent across space” (Wood et al., 2002, p. 314). Although several sedimentological and surface characteristics were considered, desert pavement mosaics were primarily differentiated from bare ground as having more than 65% of the ground covered by clasts.

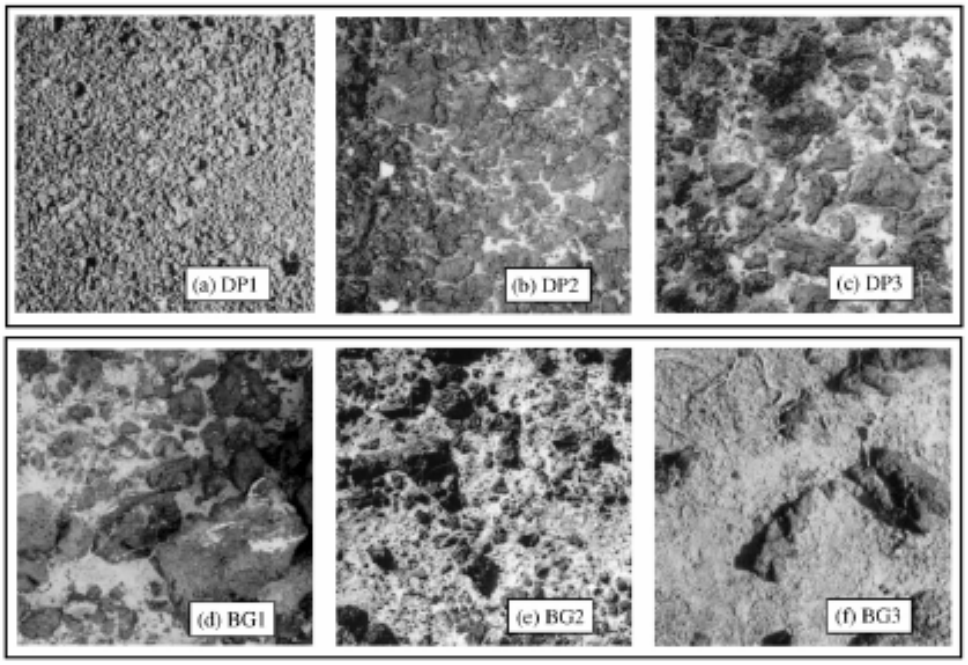

Fig. 5. Desert pavement classification system. Examples of the three defined desert pavement surface mosaics (DP1, DP2, DP3) and three bare ground surface mosaics (BG1, BG2, BG3) as classified by Wood et al., (2002). Plan view photos show desert pavement from the Cima Volcanic Field in the eastern Mojave Desert, with a 50cm field of view (Wood, 2002).

The above study in the Mojave Desert concluded that DP1 has successively more ground cover, better sorting, and smaller clasts than DP2 or DP3. Areas of desert pavement labeled as DP1 were limited in distribution, while DP2 was found more widely throughout the pavement field, and DP3 covered about half of the study site. The authors suggest that the textural variations may result from differences in their formation, with DP1 possibly indicating a regenerative surface that has been covered by gravels and DP2 forming according to the accretionary mantle model. Textural differences among desert pavements seen during the authors' field reconnaissance in other arid lands suggest that this surface mosaic type classification may be effective when applied to diverse geomorphic surfaces.

Further studies by Wood et al. (2005) suggest that these distinct surface mosaics could also correspond to fundamental characteristics of vegetation and soil morphology in the desert pavement areas. DP2 and DP3 are characterized by less than 5% shrub cover, with DP1 exhibiting no vegetation cover. Depth of leaching and concentration of soluble salts becomes shallower with increasing degree of clast cover. Vesicular soil horizons are present in all DP mosaics, but range in thickness from 6 cm beneath DP1 to less than 2 cm at DP3. Argillic soil horizons and gypsum are typically found below vesicular soils in all three DP mosaics.

REGIONAL SETTING

3.1 Geology and Geomorphology

BBNP, Texas comprises approximately 3250 km^2 of federal lands managed by the National Park Service and is located about 425 km southeast of El Paso, Texas and 450 km west of San Antonio, Texas. This park was named after the curve, or "big bend," in the Rio Grande River that delineates the boundary between Texas and Mexico and also marks the southern extent of BBNP. Positioned along the eastern edge of the Basin and Range Province, BBNP lies at the junction of two major mountain ranges, the Rocky Mountains and the now-buried Ouachita Mountains. Big Bend National Park is situated at the heart of the Chihuahuan Desert, an area that covers 32% of the North American arid region (Tchakerian, 1997).

The following geologic narrative is based primarily on the work of Maxwell, 1966; 1968; and Maxwell et al., 1967. The diverse geologic history of the Big Bend region is reflected in its stratigrafic column (Fig. 6). During the Paleozoic, a deep-sea trough extended through the Big Bend area, which accumulated sediments eroded from the highlands. These sand, gravel, and clay deposits of the late Paleozoic are still visible at the surface in the northern portion of the park. The Ouachita orogeny of the Pennsylvanian Period deformed the sedimentary rocks of the Ouachita System, which are exposed in BBNP, and initiated a grand period of denudation which formed thick beds of Mesozoic sandstones, shales, and limestones. Then, a warm, shallow sea of the Cretaceous Period deposited limestone and mudstone layers throughout the region, and

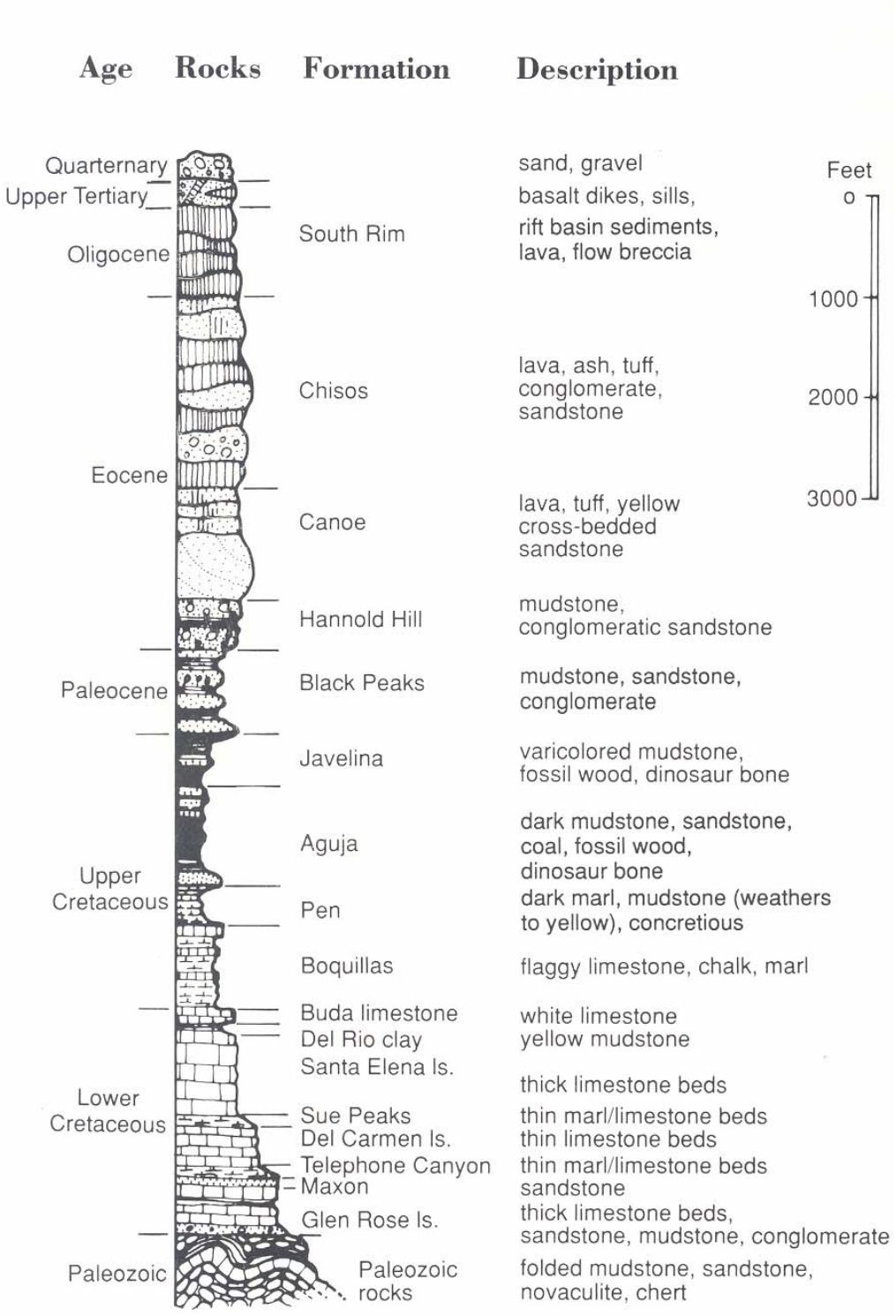

Fig. 6. Stratigraphic column of geology in Big Bend National Park. (Nelson, 1992)

sandstones and siltstones were left behind as the sea retreated to its present position. The Laramide orogeny during the late Cretaceous was the second major orogeny to affect BBNP, leading to the formation of the Mariscal Mountains of BBNP, the most southern extension of the Rocky Mountains in the United States. A discontinuous series of Tertiary volcanic activity during the Eocene and Oligocene Periods formed the Chisos Mountains, caused lava to flow west and southwest of the Chisos Mountains, and left behind numerous igneous intrusions and layers of tephra. Throughout the Quaternary, weathering and erosion has left behind thick alluvial and colluvial deposits including basin fill, consolidated gravel, alluvial fans, talus, and stream deposits, covering approximately one-fourth of the park (Maxwell et al., 1967).

The present geomorphic setting of BBNP, shown in Appendix A, is largely the result of Cenozoic deformation and subsequent weathering, erosion and fluvial activity, combined with volcanism associated with the formation of the Basin and Range Province (Tchakerian, 1997). The oldest rocks in BBNP are exposed on the park's north side near Persimmon Gap, where Paleozoic rocks of the Ouachita system were thrust over Cretaceous limestones. The Chisos Mountains, at Big Bend's center, are the product of extrusive lava flows, breccias, and rhyolites which overlie the intrusive igneous mass that forms the base of the mountains. Geomorphologically, the entire central portion of the park, including the Chisos Mountains, is a down-dropped block (graben), the result of extensional faulting in the late Tertiary, and a classic example of the basin and range topography evidenced throughout much of the southwestern United States. BBNP's southeastern side is dominated by exposed Cretaceous sedimentary

rocks and alluvial fan deposits sloping away from the Chisos Mountains. The Rio Grande River cuts through a thick section of the Santa Elena limestone at Boquillas Canyon. Aeolian deposits, mostly in the forms of climbing dunes, are also located in the southeast section of BBNP. The western part of BBNP (the focus of this study) has been mapped as Quaternary surficial deposits of alluvium or gravel and silt. Volcanics of the Chisos formation including ashbeds, tuffaceous clays and sandstones, basaltic and rhyolitic lavas, and igneous intrusions are also evidenced in this area. Badlands are found along Old Maverick Road where Cretaceous clay beds have been eroded by the Alamo Wash, Javelina Wash, and Dawson Creek (Spearing, 1991).

The USGS (2004) is currently undertaking the re-mapping and production of a digitized geologic map of BBNP to replace Maxwell's outdated 1967 version. Large unmapped areas of Quaternary surficial deposits are serious gaps in knowledge, and the USGS hopes that detailed mapping of these surficial deposits (including desert pavements) will lead to a better understanding of the Quaternary geologic history of BBNP.

3.2 Modern Climate

The aridity of the Chihuahuan Desert is attributed to the rainshadow effect of the Sierra Madre Occidental and Sierra Madre Oriental mountain ranges, the subtropical high and continentality (Tchakerian, 1997). Five National Climatic Data Center weather stations are scattered throughout BBNP (Fig. 7). The mean annual precipitation in the Big Bend National Park is about 400 mm (15 in), which falls mainly during the summer

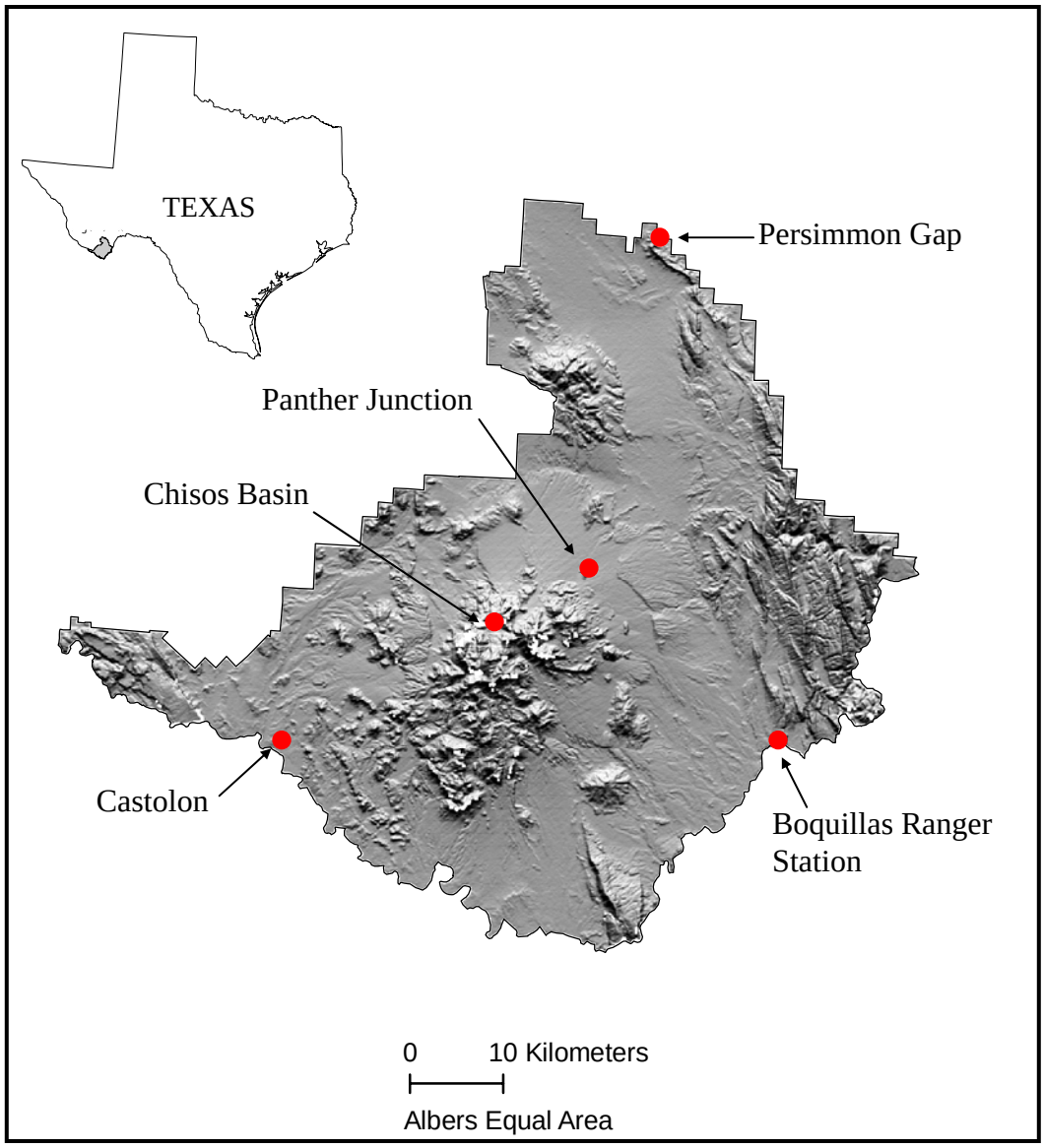

Fig. 7. Location of weather stations in Big Bend National Park (Image adapted from Herbert, 2004).

monsoon season. As Table 1 shows, however, the precipitation and temperature values vary greatly throughout the park because of elevation, with the high Chisos mountains experiencing considerably more precipitation and cooler temperatures than the adjacent desert piedmonts and the Rio Grande floodplains. The Castolon and Panther Junction weather stations (Fig. 8), located nearest the desert pavement study areas, are indicative of a BWh (dry and arid with hot summers) Köppen climate classification (Herbert, 2004).

Table 1. Climate variations throughout Big Bend National Park. Temperature and precipitation values reported in Herbert (2004)

Station Name	Cooperative Station Identifier	Elevation (m)	Mean July temperature (°C)	Mean Jan. temperature (°C)	Mean annual precip. (mm)
Boquillas Ranger Station	410950	566.3	30.4	9.2	251
Castolon	411524	661.1	31.2	10.4	249
Persimmon Gap	416959	873.3	29.1	9.3	236
Panther Junction	416792	1140.0	27.3	9.4	362
Chisos Basin	411715	1615.4	23.4	8.3	487

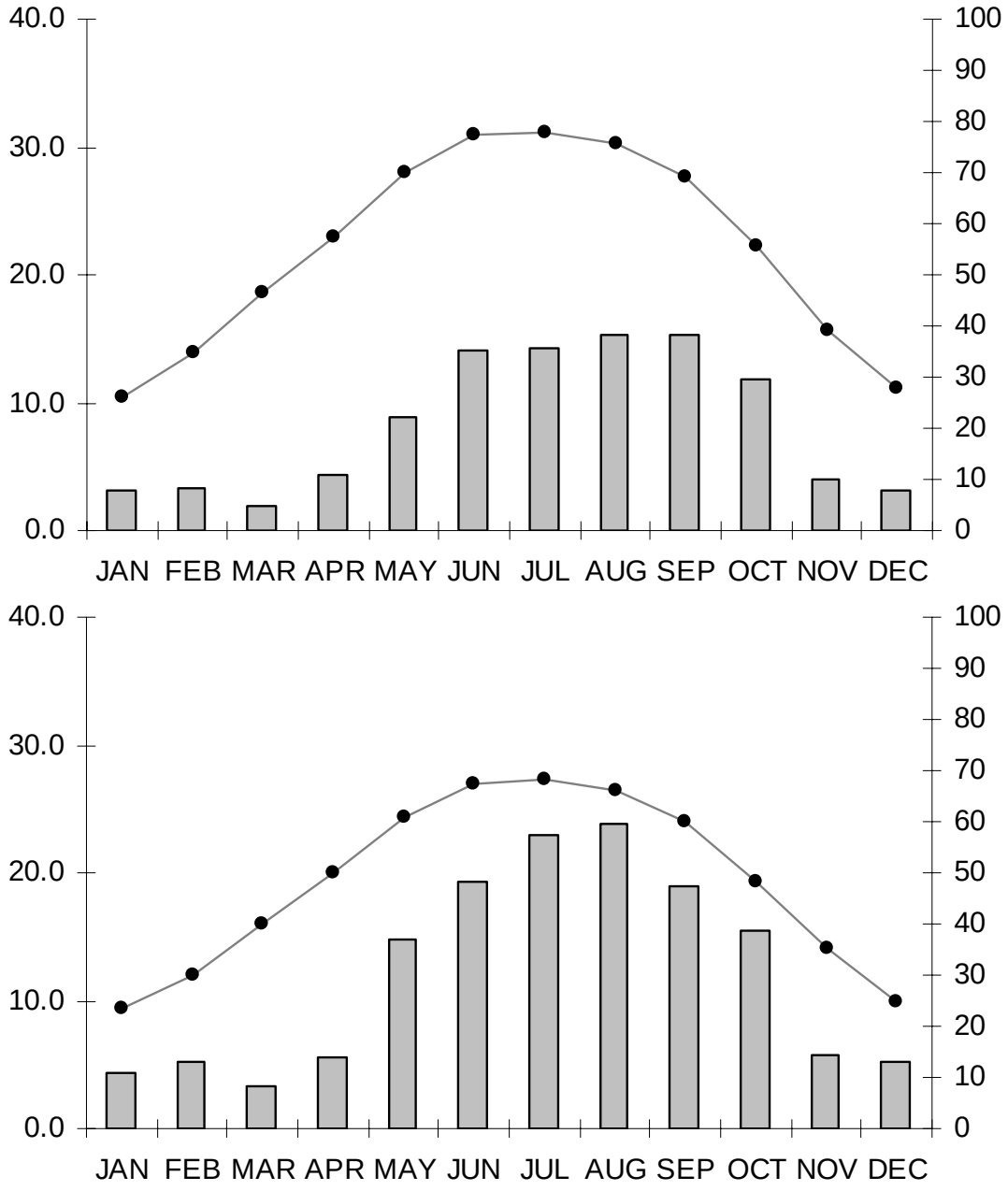

Fig. 8. Climographs for Castolon and Panther Junction weather stations. Castolon (top) is located ~15 km from study area 1 and study area 2. Panther Junction (bottom) is located ~5 km from study area 3. Temperatures are in ^{o}C (line, left axis) and precipitation in mm (bars, right axis). Data from 1971-2000 National Climatic Data Center climate normals (Herbert, 2004).

RESEARCH DESIGN AND METHODS

4.1 Study Areas

The mapping of desert pavement distribution was accomplished following consultation with park scientists, analysis of geologic maps and digital imagery, and field reconnaissance. The most well-developed desert pavements were found to be on abandoned alluvial apron surfaces in the western section of BBNP. From this section, three desert pavement study areas (Fig. 9) representing the diversity of desert pavements in the park were selected for detailed geomorphological analysis: Study Area 1 off Old Maverick Road, Study Area 2 off Ross Maxwell Scenic Drive, and Study Area 3 off Croton Springs Road.

Each area is visually distinct and situated in a different geomorphic setting (Fig. 10 and Fig. 11). The desert pavement at Study Area 1 has more rounded clasts, sparse vegetation, and is located near the badlands formed by the Alamo and Javelina Washes. The desert pavement at Study Area 2 contains poorly sorted angular clasts and is surrounded by intrusive igneous formations and other volcanic deposits. Study Area 3 exhibits a steeper slope, is more densely vegetated than the other two sites, and has weathered, mosaiced clasts.

For each study area, nine $1m^2$ sample sites of desert pavement spaced 15 meters apart along three parallel transects were selected and their GPS locations recorded using a handheld Garmin device. Where vegetation prevented placing the $1m^2$ grid directly on the pavement, the grid was relocated immediately next to the plant. For simplicity, the

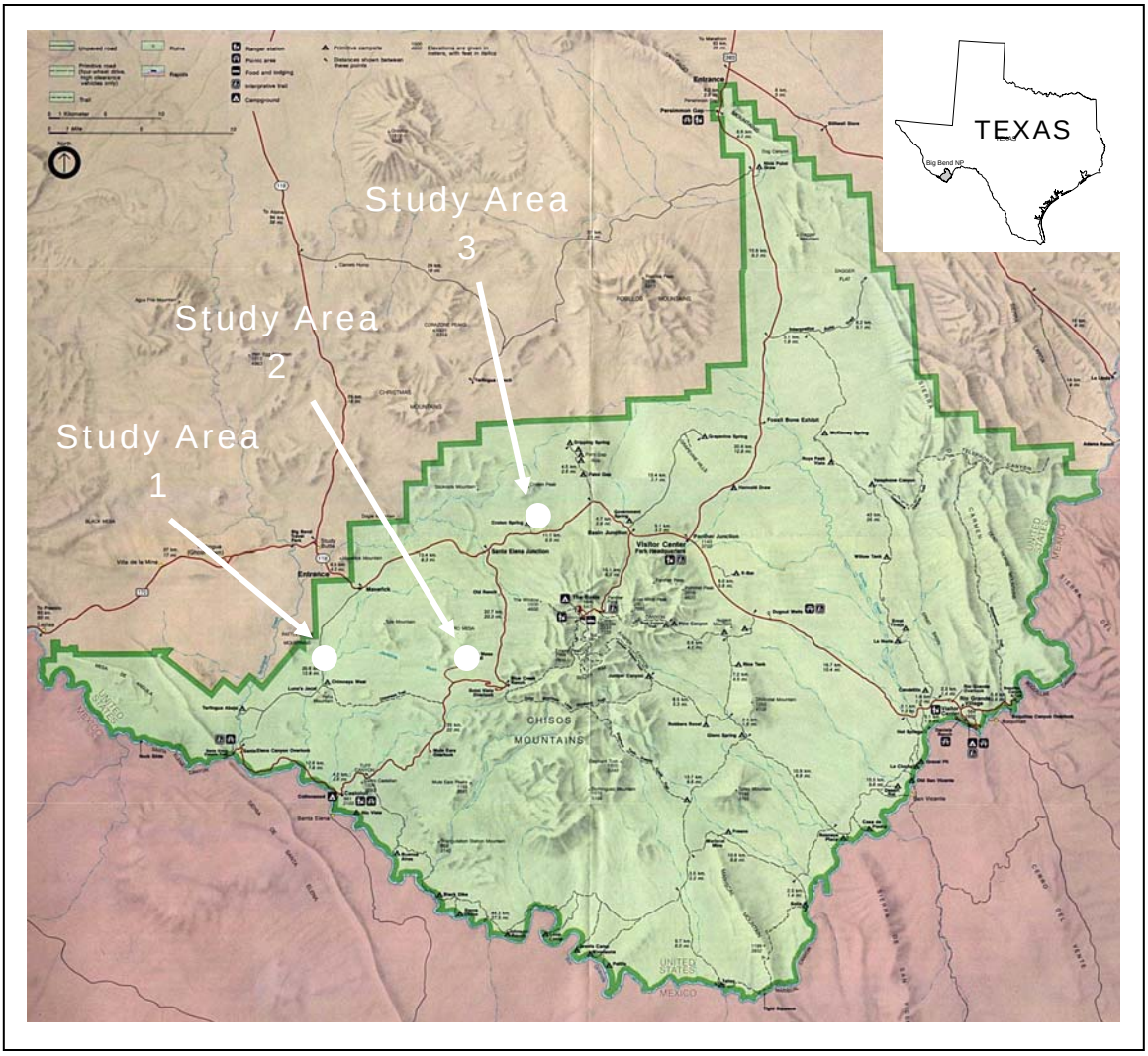

Fig. 9. BBNP map showing three desert pavement study areas. The western section of the park was determined to be optimal for desert pavement development. Image modified from National Park Service (2006).

Fig. 10. Landscape views of desert pavement study areas.
(Top) Study Area 1 off Old Maverick Road
(Center) Study Area 2 off Ross Maxwell Scenic Drive
(Bottom) Study Area 3 off Croton Springs Road

Fig. 11. Close-up views of desert pavement study areas.
(Top) Study Area 1 off Old Maverick Road
(Center) Study Area 2 off Ross Maxwell Scenic Drive
(Bottom) Study Area 3 off Croton Springs Road

sample sites will be referred to by their site number, with a dash separating the Study Area number from the sample site number (e.g. sample site 2-8 is the 8th sample site at Study Area 2, off Ross Maxwell Scenic Drive). In order to accomplish the four objectives outlined earlier, the following field and laboratory methods were conducted.

4.2 Field Sampling

At each sample site, two digital photographs were taken for later analysis: one of the ground cover, and one with a 1 m^2 grid with string intersections placed at 10 cm intervals. Appendix B contains sample site photographs from Study Areas 1, 2, and 3. Using a list of ten randomly generated numbers, the surface clasts ($\geq$ 4 mm in diameter) located nearest each corresponding numbered grid intersection were collected. After removing all surface clasts from a 10 cm^2 area, a 100 gm sediment sample was taken from the top 2 cm immediately beneath the desert pavement. At three sample sites in each study area, a 10 cm deep soil cross-section was dug, photographed, and described ─ taking care to note vesicular horizon depth and degree of development, depth to argillic horizon, and character of other visible subsoils. In addition, a 100 gm soil sample was collected at 10 cm depth from one randomly selected sample site within each study area (1-5, 2-4, and 3-7). After completing the field sampling, geologic handsamples were collected from surrounding outcrops, and the direction and percent slope of the desert pavement study area, the relative abundance of vegetation types, and the approximate degree of vegetative cover were recorded. This procedure was repeated at all three study areas.

4.3 Determining Desert Pavement Classification

For each sample site, clast diameter along the b-axis was recorded for the 81 surface clasts nearest the string intersections (9 x 9) on the gridded photographs using the measuring tapes in the photos. Following procedures outlined in Wood et al., (2002), clast size was recorded to the nearest millimeter, and only clasts greater than 4 mm along the b-axis were considered as surface clasts for size analysis. Mean, median, mode, maximum and minimum clast sizes were calculated for each sample site. Sorting of the desert pavement surface clasts was determined from the standard deviation of the clast sizes (converted to cm), where sample sites with values below 1 were moderately sorted and values above 1 were poorly sorted (Folk, 1980). Percentage diagrams for estimating composition by volume were used to visually approximate the percent of ground covered by desert pavement clasts in the non-gridded photographs of each $1m^2$ sample site (Compton, 1985, p. 366). These values for clast size, sorting and percent cover were compared to the parameters set forth in Wood et al. (2002) to classify the desert pavement sample sites into surface mosaic types (DP1, DP2, DP3, BG1, BG2, BG3) shown in Fig. 5.

4.4 Determining Geologic Composition

The geologic composition of the desert pavement clasts was determined by visual examination of a freshly broken surface of the ten desert pavement clasts that were collected from each sample site. The dominant lithologies were compared to geologic hand samples taken from surrounding outcrops and exposed bedrock to see if the clasts

might be derived locally. Published geologic maps of the park were used to determine source when the pavement clasts did not appear to be coming from adjacent outcrops.

4.5 Determining Sediment and Soil Analysis

All sediment analysis laboratory procedures were conducted at the Soil Characterization Lab at Texas A&M University, Department of Soil and Crop Sciences. Following Kilmer and Alexander (1949), particle size analysis was conducted on sediment samples collected directly beneath the desert pavement clasts. Pretreatments to remove organics and carbonates were not conducted because it was determined that these constituents were not present in high enough proportions to cause flocculation in these soil samples. For each air-dried, mortar ground sample, the coarse fraction (>2 mm) was separated from the fine fraction by dry sieving, and the weight of both fractions was recorded. In a sedimentation bottle, 5 ml of dispersing agent (10% sodium hexametaphosphate) was added to 10 g of the fine fraction sediment sample, and the bottle was filled 2/3 full with distilled water and shaken overnight in a reciprocating shaker. After cooling to room temperature, the suspension was brought to 400 ml volume with distilled water and stirred for approximately 2 minutes using a magnetic stirrer to ensure uniform suspension. The suspension was transferred to a water bath and timing of the sedimentation period began. A pipette was lowered 5 cm into the suspension, and a 5 ml aliquot was removed and transferred to a tared crucible at the end of both the 20 μm and 2 μm sedimentation periods. The pipetted aliquots were dried overnight at 105°F (40.6°C) and weighed to 0.1 mg accuracy. The remainder of the

solution was passed through a 300 mesh (50 μm) sieve, and the silt and clay was washed through the sieve, while retaining all the sand. The sand was dried overnight at 105°F (40.6°C), passed through the nest of sieves (1.0 mm, 0.50 mm, 0.25 mm, 0.10 mm, 0.05 mm.) and the weight of the sand fraction retained on each sieve was recorded. Percent particle size fractions were calculated using the formulae outlined by Kilmer and Alexander. The amount of gypsum and calcium carbonate equivalent in the soils was determined from samples taken at the surface and at 10 cm depth for one randomly selected sample site in each Study Area (1-5, 2-4, and 3-7) following the Chittick procedure in Singer and Janitzky (1986). The GRADISTAT program was used to determine D_{50} grain size and mean textural description (Blott and Pye, 2001).

The cross-section photographs, soil horizon depth measurements, and subsurface soil descriptions taken during field sampling were used to qualitatively characterize the nature of the soils underlying the desert pavements.

RESULTS

5.1 Desert Pavement Classification

Specific values for percent clast cover, clast size, and sorting are shown in Table 2. Classification into surface mosaic units based on clast size considered five measurements: median, mean, mode, maximum, and minimum. Table 3 shows the results of the morphological classification for each sample site. Desert pavement classifications resulting from the three individual parameters above were considered, yielding either a consistent, or inconsistent, overall surface mosaic unit designation for each sample site.

5.1.1 Desert Pavement Classification for Study Area 1

Percent clast cover was more than 95% for all nine sample sites at Study Area 1, and this site was classified as DP1. Median clast width was 11 mm, and mean clast width was 13.81 mm. Classification by clast width yielded 56% DP1, and 44% DP2. Clast sorting (standard deviation) ranged from 0.7 to 1.1, with a mean of 0.8. The Wood et al. (2002) study determined that differences in sorting at DP2 and DP3 were indistinguishable, and the standard deviation of DP1 approximated 0.8. Therefore, sorting classification yielded DP2/3 at sample site 1-8, and DP1 at the remaining 89% sites. Considering all parameters, 56% of the sample sites were consistently classified as DP1, while 44% yielded inconsistent classifications.

Table 2. Clast cover, clast size, and clast sorting for each sample site.

	Sample Site		Clast Cover	Clast Size					Clast Sorting
				Median (mm)	Mean (mm)	Mode (mm)	Maximum (mm)	Minimum (mm)	Standard deviation (cm)
			(%)						
Study Area 1	1 - 1		99	8	10.59	5	41	5	0.8
	1 - 2		97	9	12.75	5	42	5	0.9
	1 - 3		97	10	13.15	5	45	5	0.8
	1 - 4		99	13	15.21	12	36	5	0.7
	1 - 5		99	10	12.19	9	37	5	0.7
	1 - 6		99.5	14	15.79	8	49	5	0.8
	1 - 7		99	14	15.23	5	36	5	0.8
	1 - 8		97	14	17.15	5	52	5	1.1
	1 - 9		97	10	12.23	6	37	5	0.7
		Mean	***98.2***	***11***	***13.81***	***7***	***42***	***5***	***0.8***
Study Area 2	2 - 1		95	19	27.96	11	105	6	2.3
	2 - 2		93	18	24.14	6	87	5	1.9
	2 - 3		97	16	26.22	9	163	5	2.8
	2 - 4		95	26	36.70	6	115	5	3.2
	2 - 5		70	27	33.77	21	107	5	2.4
	2 - 6		97	22	29.21	14	108	6	2.2
	2 - 7		93	27	35.98	8	154	5	3.0
	2 - 8		99.5	39	46.17	47	119	8	2.6
	2 - 9		97	30	44.06	9	210	5	4.1
		Mean	***92.9***	***25***	***33.80***	***15***	***130***	***5.6***	***2.7***
Study Area 3	3 - 1		90	19	23.53	5	138	5	2.0
	3 - 2		99.5	20	24.38	9	70	5	1.6
	3 - 3		85	15	22.79	10	80	5	1.9
	3 - 4		99	25	33.05	9	95	6	2.5
	3 - 5		90	19	24.26	13	72	6	1.5
	3 - 6		70	12	15.56	9	71	5	1.2
	3 - 7		85	15	18.47	15	70	5	1.2
	3 - 8		65	10	14.17	5	53	5	1.0
	3 - 9		75	21	23.75	9	94	5	1.7
		Mean	***84.3***	***17***	***22.22***	***9***	***83***	***5.2***	***1.6***

Table 3. Surface mosaic classification considering three parameters individually and the resulting classification.

Sample Site	**By Clast Cover**	**By Clast Width**	**By Sorting**	***Using all parameters***
1 - 1	DP 1	DP 1	DP 1	*DP1*
1 - 2	DP 1	DP 1	DP 1	*DP1*
1 - 3	DP 1	DP 1	DP 1	*DP1*
1 - 4	DP 1	DP 2	DP 1	*inconsistent*
1 - 5	DP 1	DP 1	DP 1	*DP1*
1 - 6	DP 1	DP 2	DP 1	*inconsistent*
1 - 7	DP 1	DP 2	DP 1	*inconsistent*
1 - 8	DP 1	DP 2	DP 2 or DP 3	*inconsistent*
1 - 9	DP 1	DP 1	DP 1	*DP1*
2 - 1	DP 1	DP 2	DP 2 or DP 3	*inconsistent*
2 - 2	DP 1	DP 2	DP 2 or DP 3	*inconsistent*
2 - 3	DP 1	DP 2	DP 2 or DP 3	*inconsistent*
2 - 4	DP 1	DP 3	DP 2 or DP 3	*inconsistent*
2 - 5	DP 3	DP 3	DP 2 or DP 3	*DP 3*
2 - 6	DP 1	DP 3	DP 2 or DP 3	*inconsistent*
2 - 7	DP 1	DP 3	DP 2 or DP 3	*inconsistent*
2 - 8	DP 1	DP 3	DP 2 or DP 3	*inconsistent*
2 - 9	DP 1	DP 3	DP 2 or DP 3	*inconsistent*
3 - 1	DP 2	DP 2	DP 2 or DP 3	*DP 2*
3 - 2	DP 1	DP 2	DP 2 or DP 3	*inconsistent*
3 - 3	DP 2	DP 2	DP 2 or DP 3	*DP 2*
3 - 4	DP 1	DP 3	DP 2 or DP 3	*inconsistent*
3 - 5	DP 2	DP 2	DP 2 or DP 3	*DP 2*
3 - 6	DP 3	DP 2	DP 2 or DP 3	*inconsistent*
3 - 7	DP 2	DP 2	DP 2 or DP 3	*DP 2*
3 - 8	DP 3	DP 1	DP 1	*inconsistent*
3 - 9	DP 3	DP 2	DP 2 or DP 3	*inconsistent*

5.1.2 Desert Pavement Classification for Study Area 2

Eight sample sites at Study Area 2 had clast cover values between 93% and 99.5%, indicating DP1. Only 70% of the ground was covered by clasts at site 2-5 resulted in DP3 classification. Mean clast width was 33.8 mm and median clast size was 25 mm. Classification by clast width yielded 67% DP3 and 33% DP2. Clast sorting (standard deviation) ranged from 1.9 to 4.1, and 100% of the sample sites were classified as DP2/3 by sorting values. Considering all parameters, one site was consistently classified as DP3, while 88.9% of the sample sites yielded inconsistent classifications.

5.1.3 Desert Pavement Classification for Study Area 3

In Study Area 3, percent clast cover ranged from 66% to 99.5%, with a mean of 84%. Sample sites 3-2 and 3-4 (22%) were designated DP1 with clast cover of greater than 99%. Forty-four percent of the sites were classified as DP2, and the remaining 33% indicated DP3 classification by clast cover. Mean clast size for Study Area 3 was 22.22 mm, and the mean was 17 mm. Classification by clast width yielded 11% DP1, 11% DP2, and 78% DP3 designations. Clast sorting ranged from 1.0 mm to 2.0 mm, with a mean of 1.6 mm, yielding 89% DP2/3 classification and 11% DP1 classification. Forty four percent of the sample sites yielded DP2 classification using all parameters, and 56% were inconsistently classified.

5.2 Geologic Composition

Table 4 depicts the geologic composition and relative abundance of the desert pavement clasts. Establishing source rock will facilitate the better understanding of desert pavement geomorphology.

5.2.1 Geologic Composition of Study Area 1

There was not a dominant rock type at Study Area 1. Rhyolite comprised 50% of the pavement clasts, and sandstone 10%. Basalt, siltstone, quartzite, diorite, chert, granite, limestone, and shale clasts comprised less than 10% each. Most of these Study Area 1 pavement clasts were subrounded to rounded. Figure 12 shows that there were no adjacent outcrops from which to collect geologic samples, but the rock types present at Study Area 1 are depicted in the geologic map in the upstream vicinity of this desert pavement area (Maxwell et al., 1967).

5.2.2 Geologic Composition of Study Area 2

Study Area 2 pavement clasts were 94% rhyolitic, with lesser amounts of diorite and basalt. Resistant rhyolite served as a caprock for many of the high ridges surrounding this study area, and the rhyolite capstone was almost completely eroded near the pavement field. Figure 13 shows that rhyolite comprised both outcrops adjacent to the desert pavement.

Table 4. Geologic composition of desert pavement clasts.

	Rock type	**Abundance %**
Study Area 1	Rhyolite	50
	Sandstone	10
	Basalt	7
	Siltstone	7
	Quartzite	7
	Diorite	5
	Chert	5
	Granite	5
	Limestone	2
	Shale	2
Study Area 2	Rhyolite	94
	Basalt	3
	Diorite	3
Study Area 3	Basalt	96
	Sandstone	2
	Rhyolite	1
	Petrified Wood	1

Fig. 12. Desert pavement at Study Area 1 showing no adjacent outcrops.

Fig. 13. Geologic composition of outcrops adjacent to Study Area 2.

5.2.3 Geologic Composition of Study Area 3

Pavements clasts at Study Area 3 were predominately basaltic (96%). Layers of basalt, consistent with the pavement clasts, capped ridges just upslope of the desert pavement field at Study Area 3, as shown in Fig. 14. In some places, steeply tilted sandstone bedrock was exposed in the pavement field, and an adjacent outcrop consisted of sandstone.

5.3 Sediment and Soil Analysis

Table 5 shows selected characteristics of surface sediment samples collected less than 2 cm below the desert pavement for all sample sites. Detailed sediment analysis results are found in Appendix C. Surface sediment samples from all sites at the three study areas exhibited a silty (very coarse to medium silt) mean texture. The majority of samples in this study had a silt-sized median grain size. Chemical composition of surface and subsurface sediments is shown in Table 6, and changes in sediment chemical composition with depth is represented in Fig. 15.

5.3.1 Sediment and Soil Analysis at Study Area 1

Surface sediments were dominated by a mean texture of very coarse silt (67%), with 33% coarse silt. Percent fine (silt and clay) ranged from 39.7% to 59.9%, with a mean of 47% silt and clay composition. Grain size distribution graphed as cumulative percent finer (Fig. 16) at Study Area 1 appears generally consistent at all sample sites. Median grain sizes (D_{50}) ranged from 0.3 to 0.7 mm, with a mean of 0.6 mm. Comparing

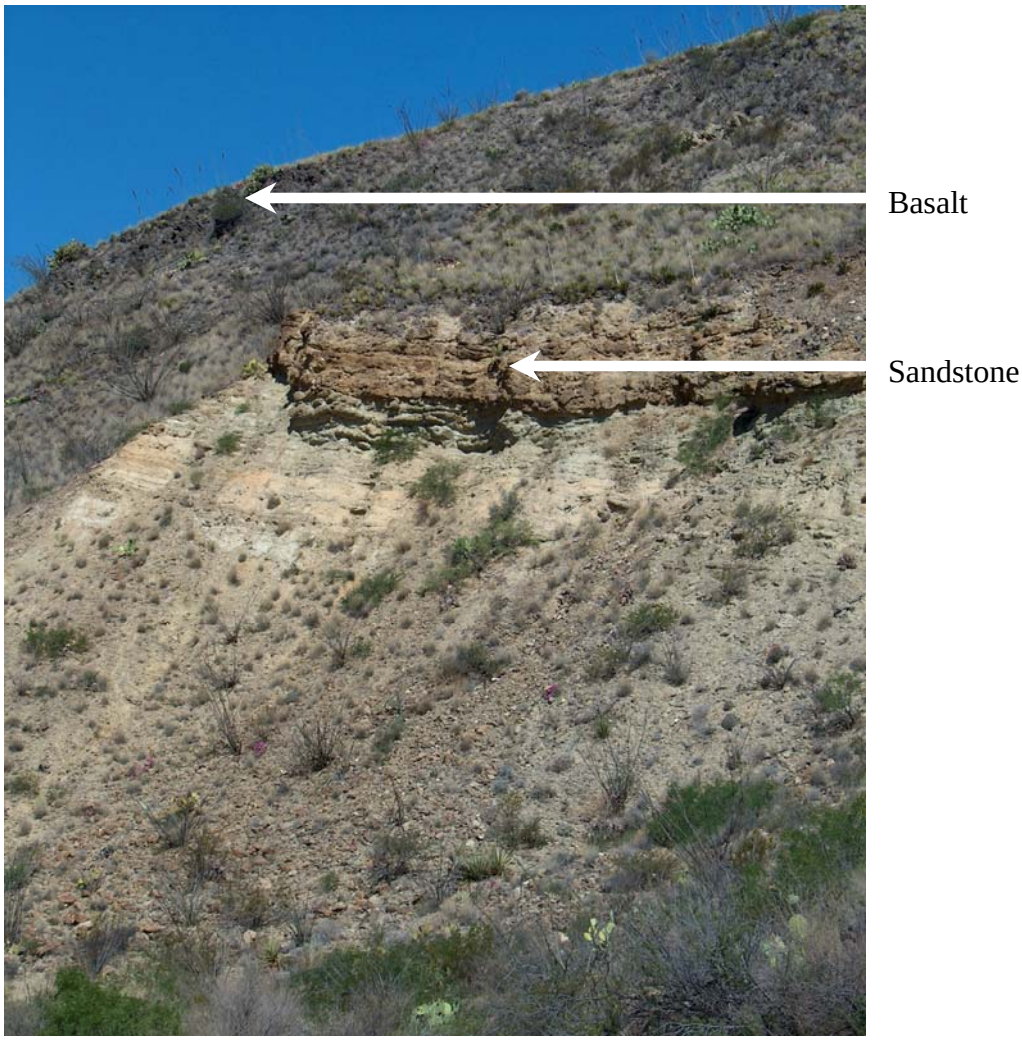

Fig. 14. Geologic composition of outcrops adjacent to Study Area 3.

Table 5. Analysis of sediment 2 cm beneath desert pavement.

	Sample Site	D_{50} Grain Size (mm)	Mean Textural Description	Percent Composition Silt	Percent Composition Clay	Percent Fine (Silt + Clay)
Study Area 1	1-1	0.06	Very Coarse Silt	34.9%	9.4%	44.3%
	1-2	0.07	Very Coarse Silt	31.7%	9.0%	40.7%
	1-3	0.07	Very Coarse Silt	32.3%	9.7%	42.0%
	1-4	0.05	Very Coarse Silt	36.3%	11.9%	48.2%
	1-5	0.05	Very Coarse Silt	39.2%	9.9%	49.1%
	1-6	0.07	Very Coarse Silt	28.2%	11.5%	39.7%
	1-7	0.03	Coarse Silt	44.4%	15.5%	59.9%
	1-8	0.05	Coarse Silt	35.0%	15.2%	50.2%
	1-9	0.05	Coarse Silt	34.4%	14.7%	49.1%
	Mean	***0.06***		***35.2%***	***11.9%***	***47.0%***
Study Area 2	2-1	0.08	Very Coarse Silt	25.3%	13.7%	39.0%
	2-2	0.07	Very Coarse Silt	23.4%	19.7%	43.1%
	2-3	0.02	Coarse Silt	31.8%	30.2%	62.0%
	2-4	0.06	Very Coarse Silt	25.8%	21.6%	47.4%
	2-5	0.01	Medium Silt	32.8%	35.0%	67.8%
	2-6	0.06	Very Coarse Silt	30.2%	16.7%	46.9%
	2-7	0.06	Very Coarse Silt	30.5%	15.4%	45.9%
	2-8	0.01	Medium Silt	41.9%	30.4%	72.3%
	2-9	0.04	Coarse Silt	31.0%	21.6%	52.6%
	Mean	***0.04***		***30.3%***	***22.7%***	***53.0%***
Study Area 3	3-1	0.07	Coarse Silt	25.1%	15.8%	40.9%
	3-2	0.06	Coarse Silt	19.1%	27.3%	46.4%
	3-3	0.07	Coarse Silt	18.1%	20.5%	38.6%
	3-4	0.04	Coarse Silt	24.3%	28.0%	52.3%
	3-5	0.07	Very Coarse Silt	23.0%	15.0%	38.0%
	3-6	0.08	Very Coarse Silt	20.2%	15.8%	36.0%
	3-7	0.05	Coarse Silt	19.8%	28.7%	48.5%
	3-8	0.11	Very Coarse Silt	14.3%	18.5%	32.8%
	3-9	0.07	Coarse Silt	20.2%	17.1%	37.3%
	Mean	***0.07***		***20.5%***	***20.7%***	***41.2%***

Table 6. Chemical composition of surface and subsurface sediments.

Sample site	Sample depth	Calcite %	Dolomite %	$CaCO_3$ equivalent %	Gypsum %	Organics (carbon) %
1-5	2 cm	6.1	0.5	6.6	0.0	0.79
1-5	10 cm	14.7	0.6	15.5	0.0	1.80
2-4	2 cm	3.5	0.5	4.0	0.0	0.47
2-4	10 cm	……. *destroyed during lab analysis.*…….				
3-7	2 cm	6.3	0.8	7.2	0.0	0.84
3-7	10 cm	6.9	1.6	8.6	19.4	0.99

* small sample size due to NPS sampling limitations

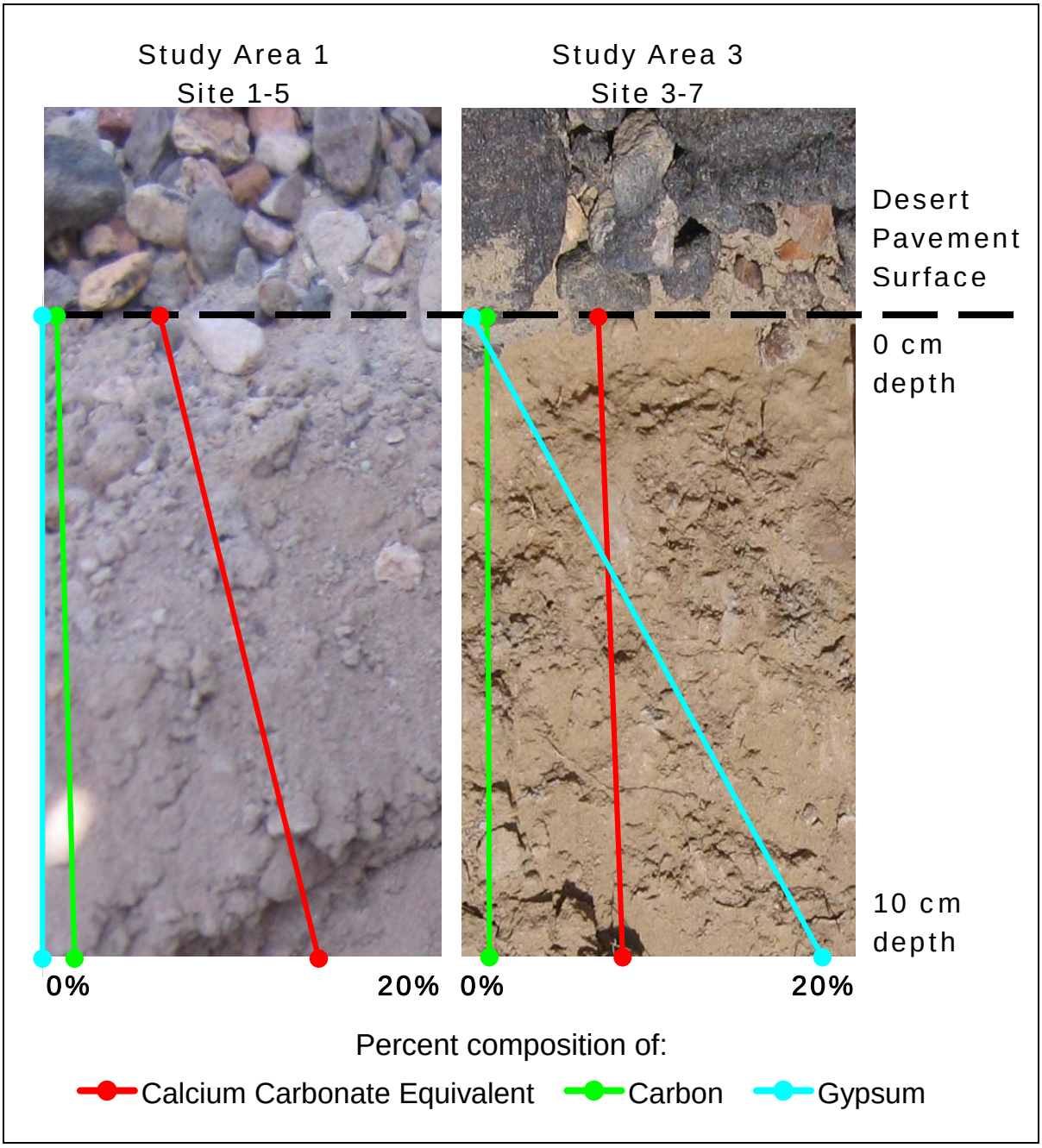

Fig. 15. Sediment chemical composition changes with depth. Percent composition of calcium carbonate equivalent, carbon, and gypsum present in sediment samples (surface and 10 cm depth) for Study Area 1 and Study Area 3. The depth sample from Study Area 2 was destroyed before lab analysis.

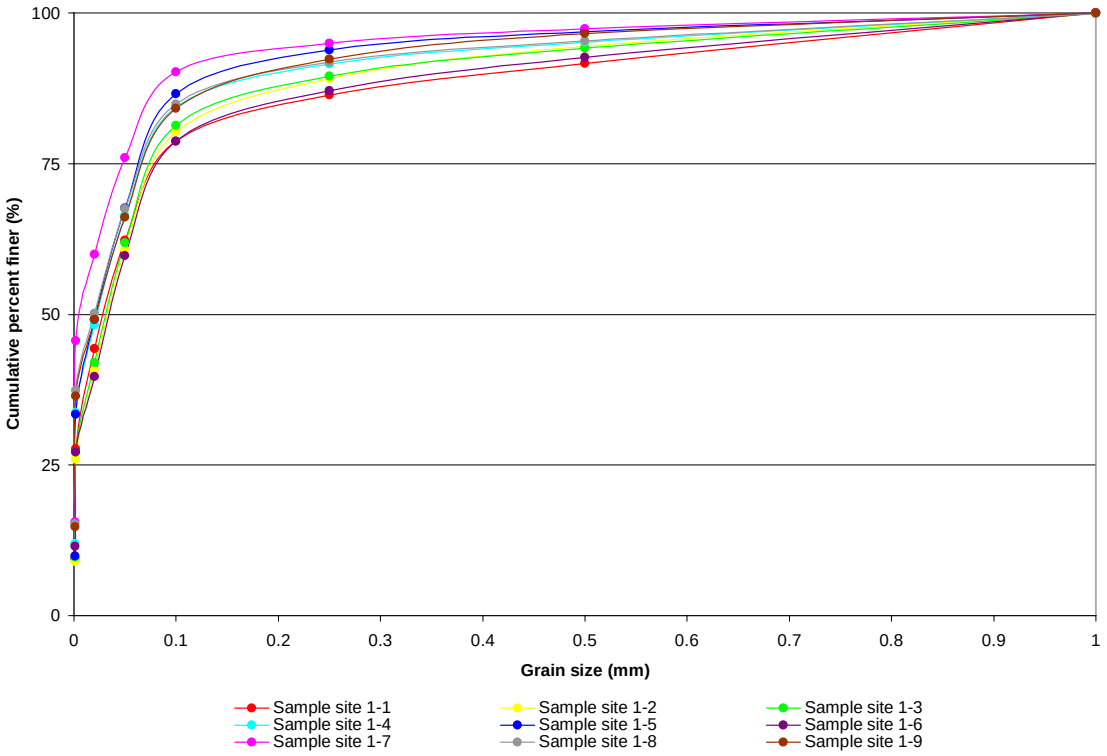

Fig. 16. Grain size distribution of Study Area 1 sediments, BBNP.

surface to subsurface sediments, cumulative percent finer distribution (Fig. 17) showed a larger percentage of coarser sediments at 10cm depth and greater amounts of fine sediments at the surface. Percent calcium carbonate equivalent (calcite plus dolomite) increased from 6.6% at the surface to 15.5% at 10 cm depth, the most significant increase with depth of all study areas. Sediments contain no gypsum, and the surface sample contained 0.79% organics and 1.80% organics at depth.

As shown in Fig. 18, cross-sections of the soil beneath the desert pavements at all three Study Area 1 sites revealed uniform sandy/silty alluvium to 10 cm depth. Sub-angular gravels 3-4mm in width comprised approximately 25% of the subsurface soils, with partial or complete calcium carbonate coatings on larger gravel grains. A well-developed vesicular soil horizon (Fig. 19) was visible to 3 cm beneath the desert pavement surface at sites 1-1 and 1-5. The vesicular soil horizon extended to 5.5 cm depth at site 1-9.

5.3.2 Sediment and Soil Analysis at Study Area 2

Fifty-six percent of the surface sediments at Study Area 2 were very coarse silt, with coarse silt and medium silt comprising 22% each. Mean percent fine (silt and clay) composition was 53%, with sample site values ranging from 39% to 72.3%. The cumulative percent finer graph (Fig. 20) of Study Area 2 shows generally consistent grain size distribution at all sample sites, with an average D_{50} grain size of 0.4 mm. The surface sample contains 4% calcium carbonate equivalent, less than 1% carbon, and no

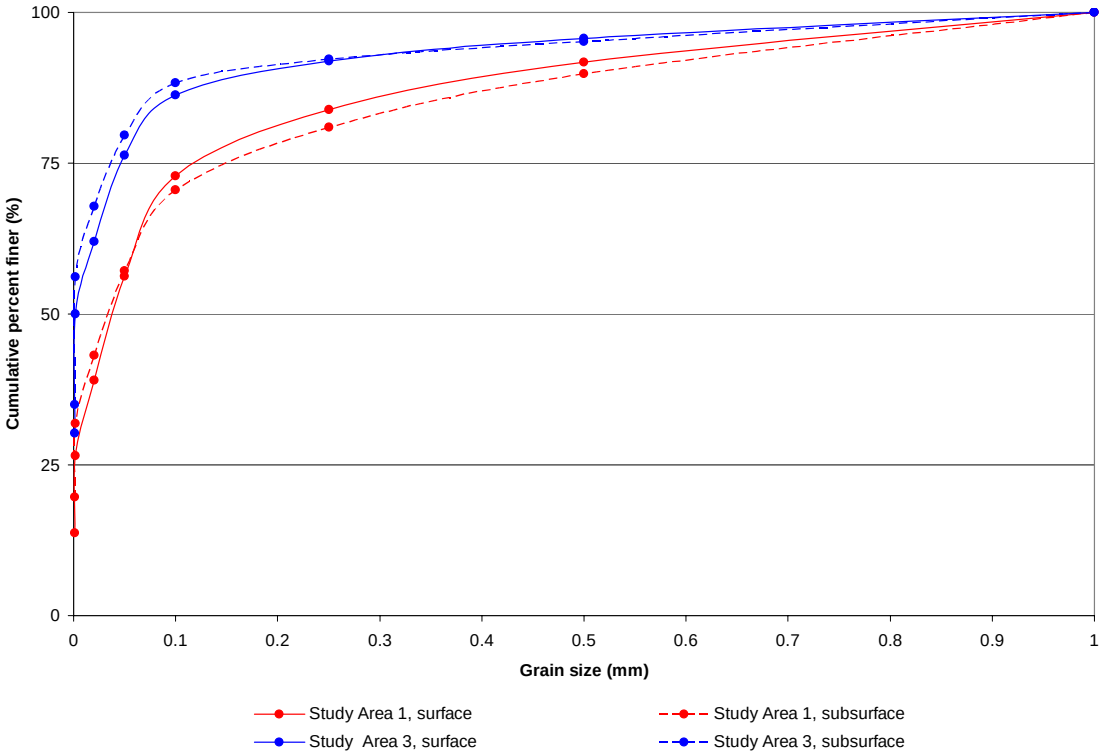

Fig. 17. Grain size distribution comparison of surface and subsurface sediments. Surface sediments sampled at 2 cm, and subsurface sediments sampled at 10 cm depth at Study Areas 1 and 3. 10cm depth sample from Study Area 2 was destroyed during lab analysis and not included in this comparison.

Fig. 18. Soil profile cross-sections (10 cm), Study Area 1. The third cross-section photograph did not develop.

Fig. 19. Soil beneath Study Areas 1 and 2. Examples of well-developed vesicular horizons at Study Area 1 (top) and Study Area 2 (bottom).

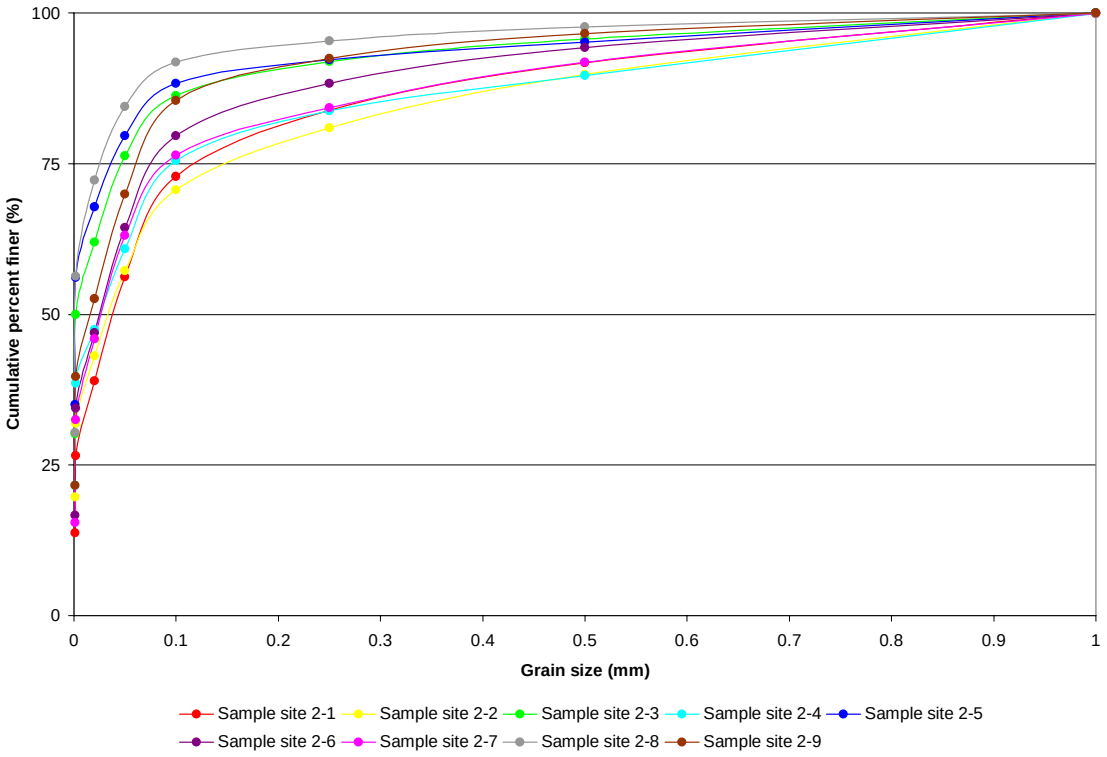

Fig. 20. Grain size distribution of Study Area 2 sediments, BBNP.

gypsum. The 10 cm depth sediment sample from Study Area 2 was destroyed during lab analysis, so surface to depth comparisons are not available.

The cross-section at site 2-1 (Fig. 21) revealed a vesicular horizon to 4.2 cm depth, underlain by clay-rich soils with a medium sub-angular blocky structure. Coarse gravels (approximately 3 cm grain size) with thin discontinuous carbonate coatings on the underside comprised 25% of the argillic soil horizon. At site 2-5, a very weakly developed vesicular horizon less than 1cm thick was underlain by virtually gravel-free clay-rich soil soils at 5 cm depth. Cross-sections at site 2-9 revealed a 1 cm thick very weakly developed vesicular horizon, and argillic soils of moderate, medium granular texture at 3 cm depth. Figure 19 shows an example of vesicular horizon at Study Area 2.

5.3.3 Sediment and Soil Analysis at Study Area 3

At Study Area 3, coarse silts dominated (67%), with 33% mean texture of surface sediments very coarse silt. Percent fine (silt and clay) ranged from 32.6% to 52.3%, with a mean of 41% silt and clay composition. Study Area 3 exhibits the most tightly constrained grain size distribution when graphed as cumulative percent finer (Fig. 22), with a mean D_{50} grain size of 0.7 mm. Comparing surface to subsurface sediments (Fig. 17), cumulative percent finer distribution showed a larger percentage of fine sediments at 10 cm depth than at the surface. Percent calcium carbonate equivalent increased from 7.2% at the surface to 8.6% at 10 cm depth. The surface sediment sample contained no gypsum, but 19.4% gypsum was present at 10 cm depth. The 10 cm depth sample at

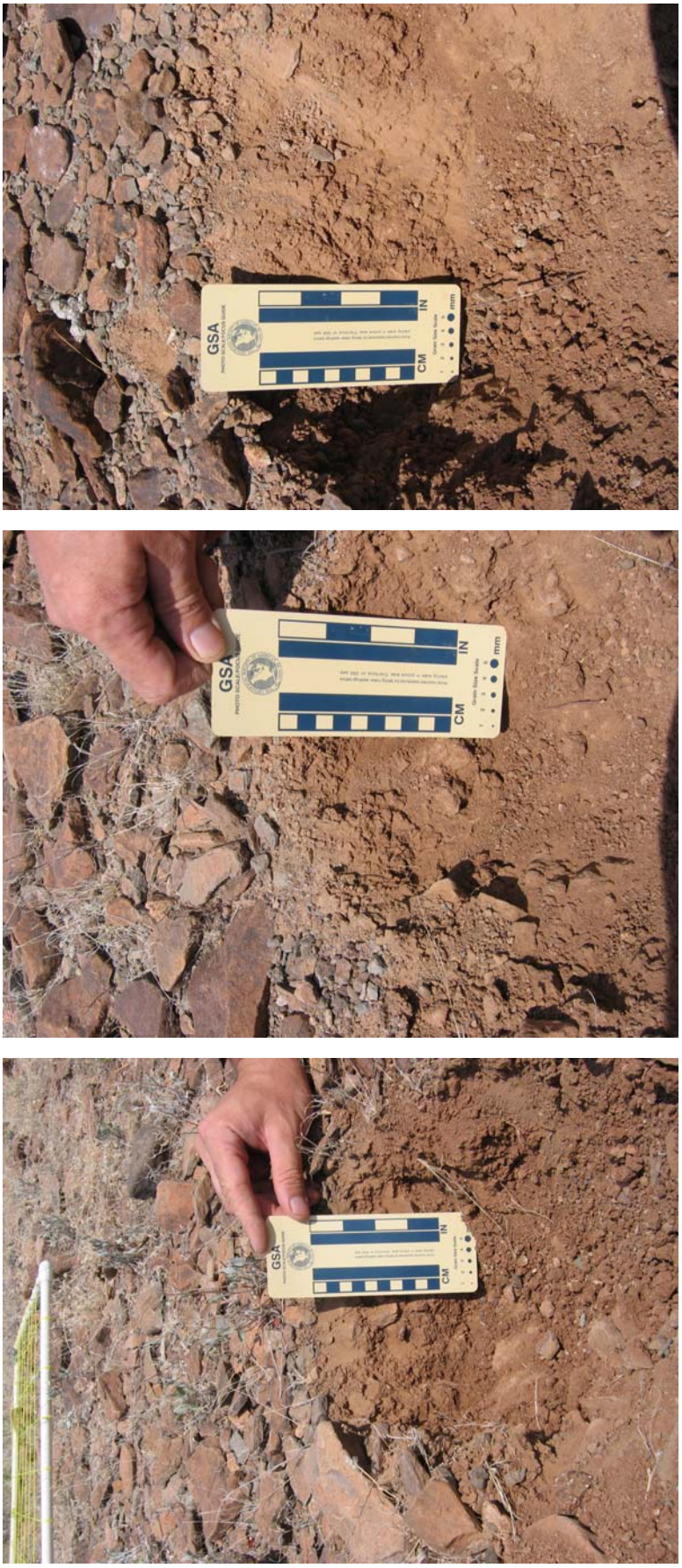

Fig. 21. Soil profile cross-sections (10 cm), Study Area 2.

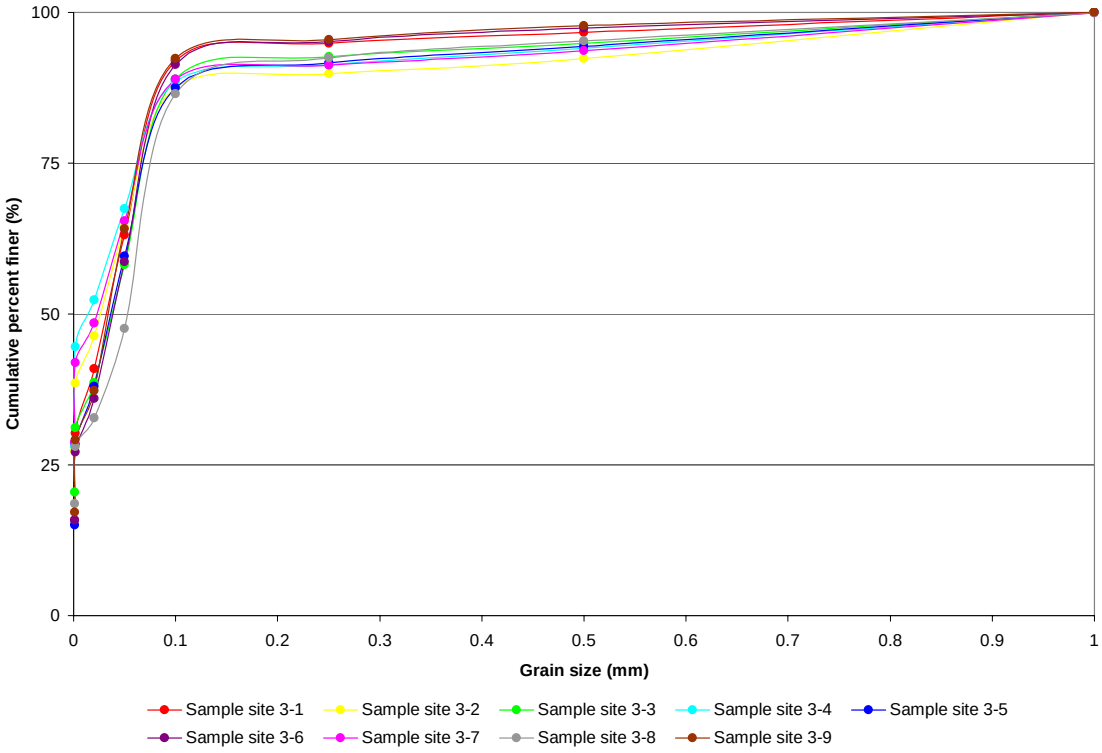

Fig. 22. Grain size distribution of Study Area 3 sediments, BBNP.

Study Area 3 contained the only gypsum present in this study. The sediment samples contained less than 1% carbon at the surface and depth.

Figure 23 shows that the cross-section at site 3-1 exhibited a weakly-developed vesicular horizon to 2 cm depth, with an argillic soil horizon at 8 cm depth. The subsurface soils contained more than 50% medium-coarse gravels with some discontinuous calcium carbonate coatings and abundant calcium carbonate nodules. Sample site 3-5 was characterized by a well-developed vesicular horizon to 3 cm depth, while a weakly-developed vesicular horizon extended to 9 cm. Argillic soils were present at 9 cm depth, and calcium carbonate nodules were abundant. Soil underlying the desert pavement at site 3-9 exhibited a discontinuous, weakly-developed vesicular horizon to 0.5 cm, becoming argillic and calcium carbonate-rich at 1.5 cm. Secondary gypsum crystals (Fig. 24) and gravels with calcium carbonate coatings on the underside were also present. Sample site 3-9 was located furthest downslope, relative to other sites at Study Area 3.

5.4 Vegetation and Slope

Landscape-scale photos, shown in Fig. 10, depict vegetation cover and slope at BBNP desert pavement study areas. Approximately 10% of the desert pavement area was vegetated at Study Area 1 off Old Maverick Road. Creosote dominated, comprising 90% of the total vegetation, along with 5% cholla, 3% ocotillo, and 2% lechugilla. Less than 1% slope was measured at this desert pavements site.

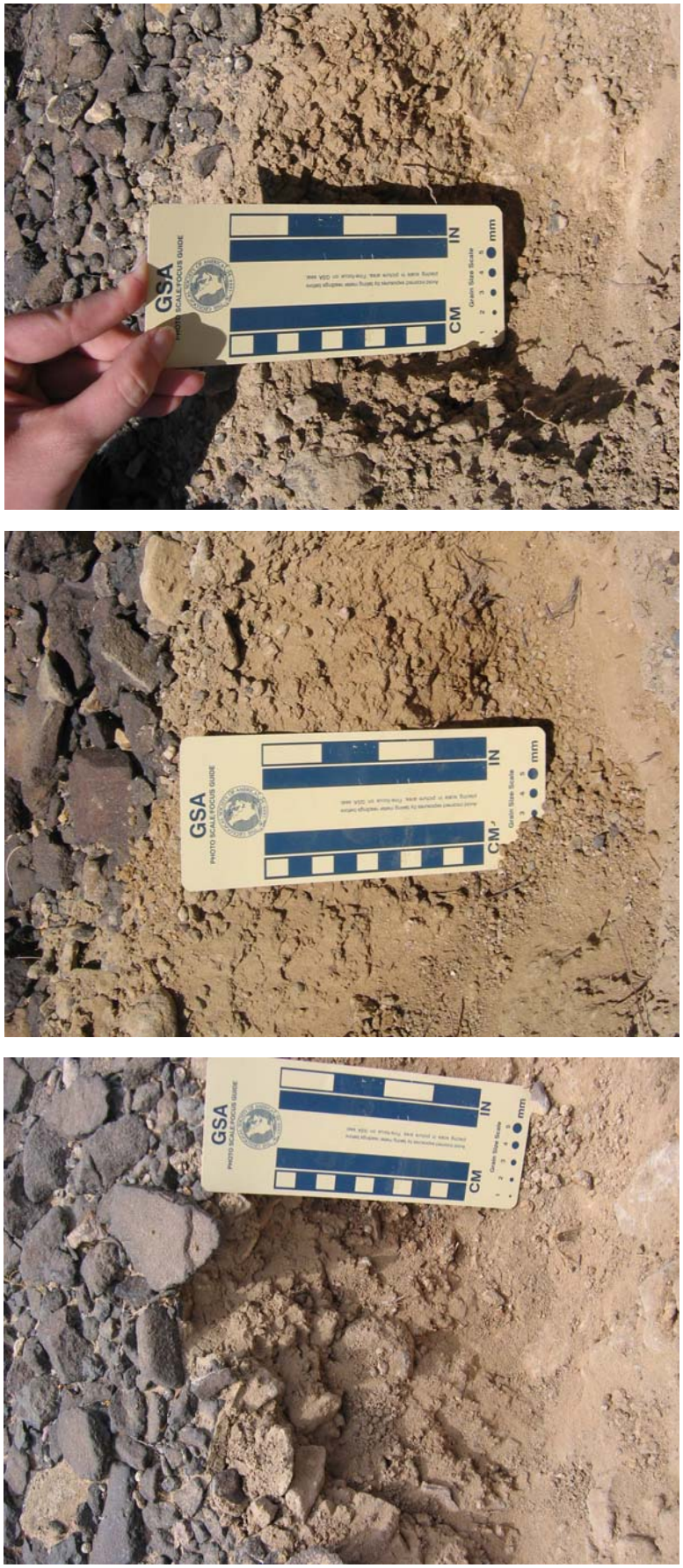

Fig. 23. Soil profile cross-sections (10 cm), Study Area 3.

Fig. 24. Soil beneath Study Area 3 desert pavement. Large secondary gypsum crystals (top). Distinct vesicles visible when a large clast was removed (bottom).

Study Area 2 off Ross Maxwell Scenic Drive exhibited 15% vegetative cover and less than 1% slope. The vegetation included approximately 80% honey mesquite, 10% cholla, and lesser amounts of creosote, prickly pear, ocotillo, annuals, and grasses.

Study Area 3 (Croton Springs Road) was the most diverse and densely vegetated desert pavement area, with approximately 30% vegetative cover: 40% creosote, 20% honey mesquite, 20% lechugilla, 10% prickly pear, and the remaining 10% ocotillo and assorted cacti. This desert pavement area had a 6% slope, the steepest of all three study areas.

DISCUSSION

6.1 Desert Pavement Distribution in Big Bend National Park

Evenari (1985) estimates that desert pavement covers more than half of the arid land surface in North America. In BBNP, that percentage is likely lower because of the presence of mountain ranges, and active fluvial and weathering processes in the park. Desert pavement formation requires a flat or moderately inclined plane surface with sparse vegetation and periods of geomorphic stability, abandonment, in order to form (Mabbutt, 1977).

Mapping of desert pavement distribution in BBNP was based on field reconnaissance, analysis of geologic maps and digital images, and discussion with park scientists. Figure 25 divides BBNP into five segments, according to the likelihood of desert pavement formation on those surfaces.

1, Green. Desert pavement is not forming in the desert plains portion of BBNP which is still covered in grasses and mesquite shrubs, owing to the cattle ranching era in BBNP's early history. The high percent of vegetative cover and active fluvial channels minimize the likelihood of desert pavement formation in the northern part of BBNP.

2, Pink. The steep slopes of the Chisos Mountains, particularly the Chisos Basin in the center of the park, would prevent the establishment of desert pavements.

3, Blue. The active floodplains of the Rio Grande are also not conducive to desert pavement formation.

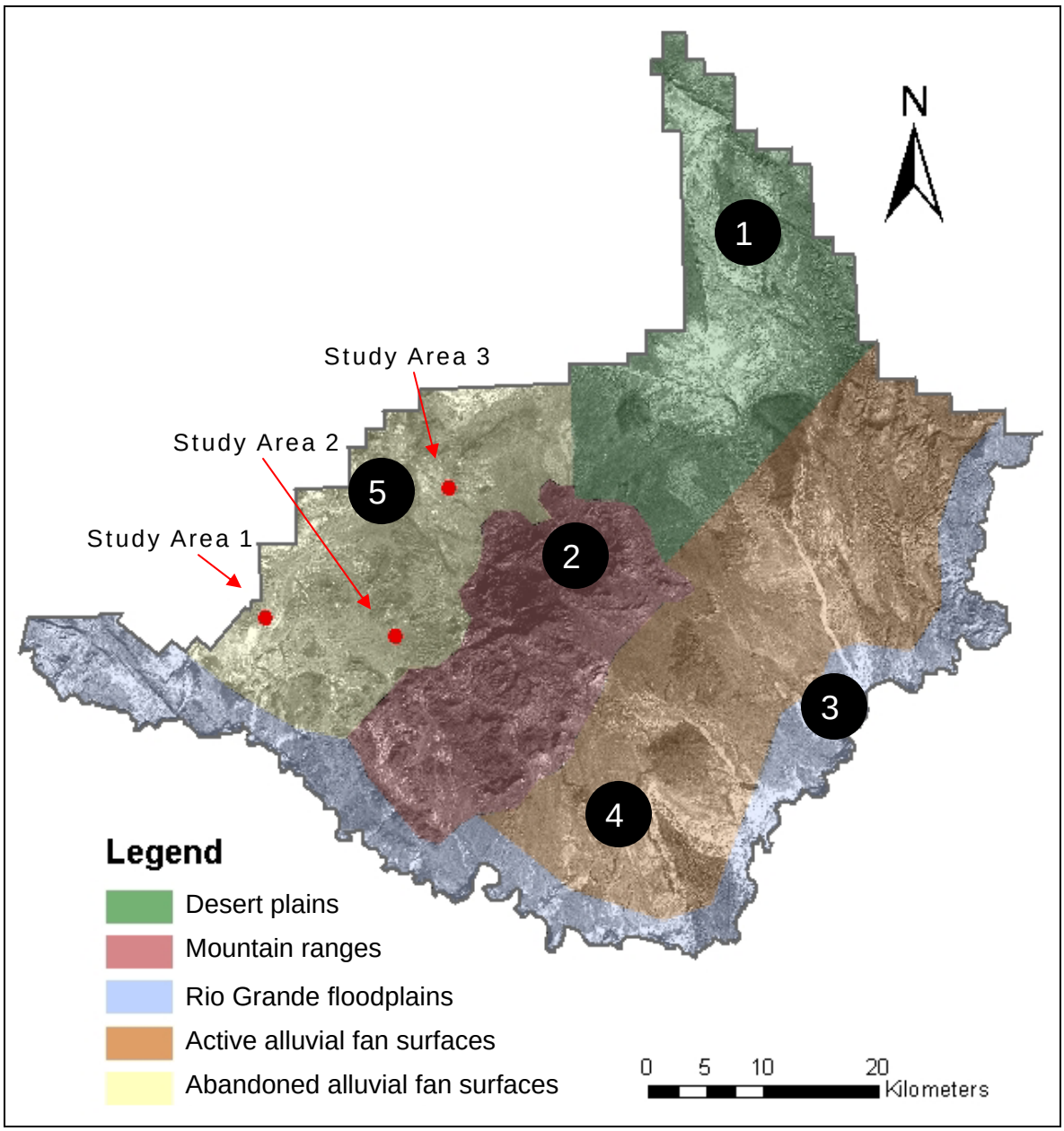

Fig. 25. Desert pavement distribution in BBNP. Three desert pavement study areas located in the western portion of BBNP, marked in red. Distribution of desert pavement in BBNP, divided into 5 segments:

1 (green)	Desert pavement NOT likely. Desert plains.
2 (pink)	Desert pavement NOT likely. Mountain ranges.
3 (blue)	Desert pavement NOT likely. Rio Grande floodplains.
4 (orange)	Desert pavement NOT likely. Active alluvial fan surfaces.
5 (yellow)	Desert pavement LIKELY. Abandoned alluvial fan surfaces.

4, Orange. Active alluvial fan surfaces prohibit pavement establishment in the southeastern portion of BBNP.

5, Yellow. Well-developed desert pavements concentrate exclusively on the abandoned alluvial fan surfaces west of the Chisos Basin in BBNP.

Vast alluvial aprons extend both to the west and southeast of the Chisos Mountain Basin, however, the processes currently acting on the two fan surfaces differ as a result of localized uplift which tilted BBNP toward the southeast direction. This tectonic activity re-activated the fan surfaces located in the southeastern portion of BBNP (4, orange), and numerous channels dissected the alluvial apron, discouraging desert pavement formation across this area. During the summer monsoon season, water flows from Chisos Basin, over the alluvial fan surfaces to the southeast, and toward the Rio Grande River.

Alluvial aprons extending west of the Chisos Basin were largely rendered inactive by the regional uplift (5, yellow). These abandoned fan surfaces are optimal locations for desert pavement formation because of their geomorphic surface stability and the decreased fluvial activity. Thick accumulations of alluvium and weathered fragments from volcanic outcrops that punctuate the fan surface act as source rocks for desert pavement clasts.

Areas where desert pavement fields may exist are extensive and difficult to access in BBNP, both because of physical and technological constraints. Few roads or trails traverse these areas, off-trail exploration in the park is regulated, and large-scale

re-mapping efforts using remotely-sensed imagery to identify desert pavement and other Quaternary surficial deposits are still ongoing by the USGS (2004).

6.2 Surface Mosaic Classification System

All of the sample sites in this study resulted in desert pavement (DP 1,2,3) classifications based on parameters of percent clast cover, clast width, and clast sorting (Wood et al., 2002). However, the classification system yielded inconsistent results in 63% of the sample sites in this study, meaning that classification from each of the three parameters did not yield the same overall result. Forty-four percent of sites at Study Area 1 were inconsistently classified, 89% at Study Area 2, and 56% at Study Area 3.

Well developed ("older") desert pavement according to this classification exhibits small, well-sorted clasts with greater percent of the ground covered by clasts. Study Area 1 contained a majority of these well-developed DP1 classified pavements, while Study Areas 2 and 3 were generally determined to be DP2 or DP3.

6.2.1 Classification by Clast Cover

The most clear distinction between the bare ground mosaics (BG 1,2,3) and desert pavement mosaics (DP 1,2,3) was found using percent ground cover; greater than 65% ground cover indicated desert pavement mosaics. In BBNP, 100% of Study Area 1 sites were DP1, and 89% of Study Area 2 were DP1. Percent clast cover varied significantly at Study Area 3, with 44% classified as DP2, 33% as DP3, and 22% as DP1.

6.2.2 Classification by Clast Width

Five clast measurements were considered when determining surface mosaic classification by clast width (median, mean, mode maximum, and minimum). In this study, median and mode values were most distinctive when determining surface mosaic classification by clast width. According to clast width parameters, 56% of Study Area 1 sample sites were classified as DP1, 67% of Study Area 2 were DP3, and 78% of Study Area 3 were DP2.

6.2.3 Classification by Clast Sorting

According to this classification system, sorting values (standard deviation) for both DP2 and DP3 were 1.3, and DP1 was well-sorted. Consequently, it was not possible to distinguish between DP2 and DP3 pavements using the parameter of clast sorting. At Study Area 1, 89% of the sites were classified DP1, while 100% of Study Area 2 and 89% of Study Area 3 were labeled as DP2/DP3.

6.3 Geologic Composition of Desert Pavement

Geologic composition of the desert pavement clasts provides the most compelling evidence for deciphering the processes involved in desert pavement formation.

6.3.1 Geologic Composition at Study Area 1

At Study Area 1, bedrock was not present, outcrops were not located nearby, and the dry washes near this study site cut through thick deposits of alluvial fill, similarly depicted on the BBNP geologic map. This region of BBNP is an alluvial apron, descending from the Chisos Mountains in west and southwesterly directions. A single rock type did not dominate the desert pavement clasts at this study area. Instead, the small, sub-rounded, well-sorted clasts of diverse geologic composition suggest that these clasts may have been derived from areas upstream. No historical flow data was collected by BBNP in these washes, and no flood events were observed during BBNP field reconnaissance. However, it is feasible that rock fragments from geologic formations upstream were entrained, weathered during transport, and deposited in their present location during a series of floods events. Desert pavement formation could have commenced subsequent to the abandonment of these wash areas.

6.3.2 Geologic Composition at Study Area 2

Bedrock was not exposed at the surface of Study Area 2, and research permit regulations in the National Park prevented disturbance beneath the desert pavement to determine depth to and composition of the underlying bedrock. However, rhyolitic pavement clasts dominated at Study Area 2 (94%), and the geologic composition was consistent with the Burro Mesa Riobeckite Rhyolite member and the Lost Mine Rhyolite member of the South Rim Formation, outcropping near the pavement field. The predominance of rhyolite at the study site can be attributed to the resistant Burro Mesa

Rhyolite, which capped many ridges throughout the area. The uppermost exposure of rhyolite was almost completely eroded adjacent to Study Area 2, contributing to rhyolitic pavement clasts.

6.3.3 Geologic Composition at Study Area 3

Steeply dipping surface exposures of sandstone bedrock were visible in some places in the desert pavement field at Study Area 3. This bedrock sandstone appears consistent with the Aguja and Javelina sandstone formations; however, only 2% of the pavement clasts in this area were sandstone. Basaltic pavement clasts dominated (96%), and the presence of geologically consistent layers of basalt upslope of Study Area 3 suggest that the clasts were likely derived from the adjacent basalt outcrop, rather than the underlying sandstone bedrock. These basalts were likely the Bee Mountain or Ash Spring Basalt members of the Chisos Formation. Study Area 3 was the most steeply sloped pavement area of the three in this study, and the basalt outcrop was located in the upslope direction of the desert pavement area, with large pieces of weathered basalt lying on the slope toward the pavement. The appearance of a black rock coating on these pavement clasts can be attributed to weathering of the basalt, rather than rock varnish.

6.4 Sediment and Soil Characteristics

Sediment samples indicated that silt, clay, and very fine sands dominate the surface sediments beneath desert pavement at all three study areas. Grain size distribution within each study area was consistent, there was little change in sediment

character with depth. Sediment analysis also revealed that variations in surface mosaic classification (DP1 versus DP2 or 3) have little or no impact on sediment size or chemical composition. National Park Service collection permit regulations necessitated the small sample sizes in this study and the disturbance of soil to only 10 cm depth.

6.4.1 Sediment and Soil Characteristics at Study Area 1

Sediments beneath the desert pavement at Study Area 1 were predominately very coarse silt, with 47% percent fine (silt and clay), and contained coarse gravels and cobbles throughout. Soil profile cross-sections showed well-developed vesicular soil horizons 3-5 cm thick forming atop uniform alluvium to 10 cm depth throughout the study area. No gypsum was present in the surface or subsurface sediment samples. This sediment character was consistent with a wash deposit, which supports the geologic composition conclusions that Study Area 1 desert pavement initially formed as a fluvial deposit. The developed nature of the soil here, relative to the other study areas, corresponds to the well-developed DP1 classification at Study Area 1.

6.4.2 Sediment and Soil Characteristics at Study Area 2

Study Area 2 sediments consisted of medium to very coarse silt with 53% percent fine (silt and clay). Soil profiles across Study Area 2 exhibited discontinuous, weakly-developed vesicular horizons atop argillic soils, owing to the clay-rich geologic formations in the vicinity. Sample sites 2-1, 2-2, and 2-4 contained slightly coarser sediments than others at Study Area 2. Sites along this transect were located closer to a

bare ground area, and increased surface runoff may have washed away fines, leaving larger sediments in the surface sample here than in other sites at Study Area 2.

6.4.3 Sediment and Soil Characteristics at Study Area 3

Coarse silts dominated sediments at Study Area 3, and weakly-developed vesicular soils were present at all sites. Gypsum was found at depth at Study Area 3 only, and secondary gypsum crystals and significant calcium carbonate accumulations were more prevalent in sites farther downslope. The steep slope of this desert pavement field may contribute to the soluble salts washing downhill and concentrating in areas with low relief.

6.5 Evaluation of Accretionary Mantle Model

Current literature favors the accretionary mantle model of desert pavement formation, which contends that desert pavement clasts are derived immediately atop bedrock and evolve *in situ* (McFadden et al., 1987). In the case of these three study areas in Big Bend National Park, however, the desert pavement clasts do not appear to have been derived from bedrock. At Study Areas 2 and 3, mechanical weathering of adjacent outcrops, and the subsequent movement of the eroded fragments downslope because of gravity or fluvial action, could serve as an alternative process of desert pavement clast derivation. At Study Area 1, deposition of clasts following flood events in nearby washes may suggest yet another preliminary stage of desert pavement formation. These

assertions are aligned with Williams and Zimbelman (1994), who suggested that sheetflood served as a precursor stage to desert pavement formation.

Predominately clay- and silt-sized surface sediments in the BBNP study areas could indicate emplacement by a combination of aeolian processes or *in situ* subsurface weathering. However, aeolian influence in BBNP is probably limited because there is little evidence of aeolian erosion and sand sources (playas or dunes) in the vicinity. In addition, subsequent soil development is not proceeding as described by McFadden et al. (1987) and Anderson et al. (1994). The characteristic vesicular soil horizon was well-developed in Study Area 1, but weakly-developed or not present at many more sites in the other study areas. The soil profiles at Study Areas 1 and 2 were not virtually stone-free, as suggested by the Mojave model. The wetter environment of BBNP may favor the formation of a soil mantle by *in situ* weathering, similar to the concentration by weathering desert pavement formation hypothesis. Differential weathering of the rhyolite and basalt at Study Areas 2 and 3 may result in differing rates of soil formation in these two areas. Despite a mature surface appearance, the desert pavements at BBNP may be “younger” than they appear.

6.6 Comparison to Desert Pavements in the Mojave Desert

Important contrasts exist between the desert pavements at Big Bend National Park and those studied in the Mojave Desert, California by Wells et al. (1985), McFadden et al. (1987), Anderson et al. (1994), Wood et al. (2002) and (2005), for example. Pavements of the Cima volcanic field are composed of bedrock-derived basalt

clasts, while the desert pavements in BBNP display varying volcanic and non-volcanic rock compositions. At the study areas in BBNP, the clasts are not likely derived from bedrock, but from other precursor stages of formation. Desert pavements at the Cima volcanic field cover vast aerial expanses of the Mojave Desert, BBNP topography results in numerous smaller fields of desert pavement. Compared to the Mojave Desert, the topography of Big Bend National Park displays more relief, with alluvial aprons descending from the Chisos Mountains, interrupted by geomorphic formations and cut by ephemeral washes. Most importantly, climate variations affect ecosystem process at the Mojave Desert and BBNP differently.

In the semi-arid environment of BBNP, it is likely that fluvial processes and enhanced (mechanical, chemical, and biological) weathering play a more prominent role in the development of desert pavement on abandoned desert surfaces than in the Mojave Desert. Results from this study indicate that fluvial processes could be responsible for the deposition of desert pavement clasts near ephemeral washes and the small-scale re-working of desert pavements surfaces in their early stages of development. The comparatively wetter climate in BBNP can contribute to greater mechanical weathering responsible for eroding outcrops and providing another source rock for desert pavement clasts. The abundance of vegetation in BBNP increases surface stability on sloping alluvial fans, which is essential to desert pavement establishment. Increased precipitation in BBNP flushes salts and carbonates deeper beneath the pavements, and increase rates of subsurface weathering of large particles, producing a soil mantle. These different environmental conditions may have also attributed to the complications in applying the

surface mosaic classification for desert pavements that was developed for the Mojave Desert. This Mojave classification system may require modification to accommodate different climatic and geomorphic regimes.

CONCLUSION

The purpose of this study was to assess the geomorphology of previously un-studied desert pavements in the Big Bend National Park, Texas, area of the Chihuahuan Desert. This geomorphic assessment filled an important gap in regional arid land literature and offered the opportunity to evaluate processes of desert pavement formation in a semi-arid environment. Specifically, this study sought to:

1) identify areas of well-developed desert pavement in BBNP and classify the desert pavements into surface mosaic units using the parameters of clast width, sorting, and percent ground cover. Well-developed desert pavements are concentrated in the western portion of BBNP because of geologic processes and subsequent geomorphic abandonment of fan surfaces. The classification system by Wood et al., (2002) yielded largely inconsistent results at the three study areas. However, the desert pavements at Study Area 1 were mostly DP1, and the other Study Areas were DP2 or DP3.

2) determine the geologic composition of the desert pavement clasts and the source rock from which the pavement was likely derived. Lithologic comparison revealed that the desert pavement clasts may have originated from stream deposits and weathering of adjacent outcrops.

3) *describe the sediments and subsurface soil horizons* that lie beneath desert pavements. Soil profiles lack the characteristics of mature desert pavements, and the underlying silt and clay sediments were most likely deposited by aeolian processes or weathered *in situ*.

4) *evaluate the applicability of the accretionary mantle model* (McFadden et al., 1987) of desert pavement formation at BBNP. Clasts derived from stream deposits and weathering of adjacent outcrops may represent precursor stages of desert pavement development to complement the accretionary mantle model developed in the Mojave Desert. Although desert pavements in BBNP are not bedrock derived, subsequent stages of soil development may begin according to the model. However, the enhanced influence of fluvial action, weathering (mechanical, chemical, and biological), and vegetation in the semi-arid environment of BBNP may contribute to variations in the stages and rates of desert pavement development. Even though desert pavements at BBNP have a well-developed surface texture, the absence of rock varnish indicates that they may be "younger" than they appear.

Since this study served as a preliminary geomorphic assessment, many avenues for future research have been uncovered. The semi-arid environment in BBNP introduces a unique set of environmental variables to the study of desert pavement in this region. Further studies could investigate the impact of vegetation on desert pavement surficial patterns. Upon completion of the USGS (2004) mapping efforts, more extensive areas of desert pavement in BBNP could be identified and included in future comparative studies. Permission from the National Park Service to expose bedrock

beneath desert pavements and to conduct comprehensive sampling in more areas could result in evidence to further substantiate these conclusions. Most importantly, Nichols et al. (2006) and Lancaster and Tchakerian (2003) note the importance of cosmogenic nuclides and luminescence dating in understanding desert surface change over time. Determining the precise age of the desert pavements in BBNP would allow for further conclusions on the stages and processes specific to the development of desert pavement at Big Bend National Park.

REFERENCES

Al-Farraj, A., Harvey, A.M., 2000. Desert pavement characteristics on wadi terrace and alluvial fan surfaces: Wadi Al-Bih, U.A.E. and Oman. Geomorphology. 35, 279-297.

Anderson, K.C., Wells, S.G., Graham, R.C., McFadden, L.D., 1994. Process of vertical accretion in the stone-free zone below desert pavements. Geological Society of America Abstracts with Programs. 26, A-87.

Belnap, J., Warren, S.D., 2002. Patton's tracks in the Mojave Desert, USA: An ecological legacy. Arid Land Research and Management. 16, 245-258.

Blott, S.J., Pye, K., 2001. GRADISTAT: A grain size distribution and statistics package for the analysis of unconsolidated sediments. Earth Surface Processes and Landforms. 26, 1237-1248.

Compton, R.R., 1985. Geology in the Field. John Wiley and Sons, New York.

Cooke, R.U., 1970. Stone pavements in deserts. Annuals of the Association of American Geographers. 60, 560-577.

Cooke, R.U., Warren, A., 1973. Geomorphology in Deserts. University of California Press, Berkeley.

Cooke, R., Warren, A. Goudie, A., 1993. Desert Geomorphology. UCL Press Limited, London.

Dixon, J.C., 1994. Aridic soils, patterned ground, and desert pavements, in: Abrahams, A.D., Parsons, A.J. (Eds.), Geomorphology of Desert Environments. Chapman and Hall, London. pp 64-81.

Dorn, R.I., 2004. Rock coating, in: A.S. Goudie (Eds.), Encyclopedia of Geomorphology, Vol. 2. Routledge, London, pp 870-873.

El-Baz, F., 1992. Preliminary observations of environmental damage due to the Gulf War. Natural Resources Forum. 2, 71-75.

Evenari, M., 1985. The desert environment, in: Evenari, M., Noy-Meir, I., Goodall, D. W. (Eds.), Hot Deserts and Arid Shrublands, Part A. Elsevier Science Publishing Company, New York, pp. 1-19.

Folk, R.L., 1980. Petrology of Sedimentary Rocks. Hemphill Publishing Company, Austin.

Haff, P.K., Werner, B.T., 1996. Dynamical processes on desert pavements and the healing of surficial disturbances. Quaternary Research. 45, 38-46.

Haff, P., 2001. Desert pavement: An environmental canary? The Journal of Geology. 109, 661-668.

Herbert, J.M., 2004. Predicting climate change in Big Bend National Park, Texas. Unpublished doctoral dissertation, Texas State University, San Marcos, TX.

Higgitt, D., Allison, R., 1999. Characteristics of stone covers on the surface of basalt flows in arid, northeast Jordan. Geomorphology. 28 (3-4), 263-280.

Hume, W.F., 1925. Geology of Egypt. Vol 1. Cairo.

Jessup, R. 1960. The Stony Tableland soils of the Australian arid zone and their evolutionary history. Journal of Soil Science. 11, 188-196.

Kade, A., Warren, S.D., 2002. Soil and plant recovery after historic military disturbances in the Sonoran Desert, USA. Arid Land Research and Management. 16, 231-243.

Kilmer, V.J., Alexander, L.T., 1949. Methods of making mechanical analyses of soils. Soil Science. 68, 15-24.

Laity, J.E., 2002. Desert environments, in: Orme, A.R. (Ed.), The Physical Geography of North America. Oxford University Press, Oxford, pp. 380-401.

Lancaster, N., Tchakerian, V.P., 2003. Late Quaternary eolian dynamics, Mojave Desert, California, in Enzel, Y., Wells, S.G., and Landcaster, N., Eds., Paleoenvironments and paleohydrology of the Mojave and southern Great Basin deserts: Geological Society of America Special Paper 368, 231-249.

Lowdermilk, W.C. Sundling, H.L., 1950. Erosion pavement, its formation and significance. Transactions of the American Geophysical Union. 31, 96-100.

Mabbutt, J.A., 1977. Desert Landforms. MIT Press: Cambridge.

Maxwell, R., 1966. Geologic map of the Big Bend National Park, Brewster County, Texas. University of Texas, Austin.

Maxwell, R.A., Lonsdale, J.T., Hazzard, R.T., Wilson, J.A., 1967. Geology of Big Bend National Park, Brewster County, Texas. University of Texas, Bureau of Economic Geology, Austin.

Maxwell, R., 1968. Big Bend of the Rio Grande: A Guide to the Rocks, Landscape, Geologic History, and Settlers of the Area of Big Bend National Park. University of Texas, Bureau of Economic Geology, Austin.

McFadden, L., Wells, S., Jercinovich, M., 1987. Influences of eolian and pedogenic processes of desert pavements. Geology. 15 (6), 504-508.

National Park Service (NPS), 2006. Big Bend National Park. <http://www.nps.gov/bibe/> Last updated Sep 13, 2006. Last accessed Oct 2006.

Nelson, K., 1992. A Road Guide to the Geology of Big Bend National Park. Big Bend Natural History Association, Paragon Press, Salt Lake City.

Nichols, K.K., Bierman, P.R., Foniri, W.R., Gillespie, A.R., Caffee, M., Finkel, R., 2006. Dates and rates of arid region geomorphic processes. GSA Today. 16 (8), 4-11.

Sharon, D. 1962. On the nature of hamadas in Israel. Geom. 6: 129–147.

Singer, M.J., and Janitzky, P., 1986. Field and laboratory procedures used in a soil chronosequence study. United States Geological Survey Bulletin. 1648, p. 49.

Spearing, D., 1991. Roadside Geology of Texas. Mountain Press Publishing, Missoula, MT.

Springer, M.E., 1958. Desert pavement and vesicular layer of some soils of the desert of the Lahontan Basin, Nevada. Soil Science Society of America Proceedings. 22, 63-68.

Tchakerian, V.P., 1997. North America, in: Thomas, D. (Ed.), Arid Zone Geomorphology: Process, Form and Change in Drylands. John Wiley and Sons, Chichester, pp. 523-542.

Tchakerian, V.P., 1999a. Dune paleoevnironments, in: Goudie, A.S., Livingstone, I., Stokes S. (Eds.), Aeolian Environments, Sediments and Landforms. John Wiley and Sons, New York, pp. 261-292.

Tchakerian, V.P., 1999b. Stone pavement, in: Mares, M.A. (Ed.), Encyclopedia of Deserts. University of Oklahoma Press, Norman, pp. 542-543.

United States Geological Survey, Turner, K.J., 2004. A new digital geologic map of Big Bend National Park, Texas. Presentation No. 47-9 2004 Denver Annual Meeting November 7-10, 2004 Geological Society of America Abstracts with Programs, 36:5, p.128.

Watson, A., Nash F., 1997. Desert crusts and varnishes, in: Thomas, D. (Ed.), Arid Zone Geomorphology: Process, Form and Change in Drylands. John Wiley and Sons, Chichester, pp. 69-107.

Wells, S.G., Dohrenwend, J.C., McFadden, L.D. and Turrin, B.D., 1985. Late Cenozoic landscape evolution on lava flow surfaces of the Cima volcanic field, Mojave Desert, California: Geological Society of America Bulletin. 96, 1518-1529.

Wells, S.G., McFadden, L.D., Poths, J., Olinger C.T., 1995. Cosmogenic ^{3}He surface-exposure dating of stone pavements: Implications for landscape evolution in deserts. Geology. 23, 613-616.

Wells, S.G., McDonald, E., Lancaster, J., Sparks, R., Johnson, W., 1998. Desert Surficial Process and Landscape Dynamics on Military Lands: Field Trip Road Log. Desert Research Institute, Reno, NV.

Williams, S.H., Zimbelman, J.R., 1994. Desert pavement evolution: An example of the role of sheetflood. The Journal of Geology. 102, 243-248.

Wood, Y.A., Graham, R.C, Wells S.G., 2002. Surface mosaic map unit development for a desert pavement surface. Journal of Arid Environments. 52 (3), 305-317.

Wood, Y.A., Graham, R.C, Wells S.G., 2005. Surface control of desert pavement pedologic process and landscape function, Cima Volcanic field, Mojave Desert, California. Catena. 59, 205-230.

APPENDIX A

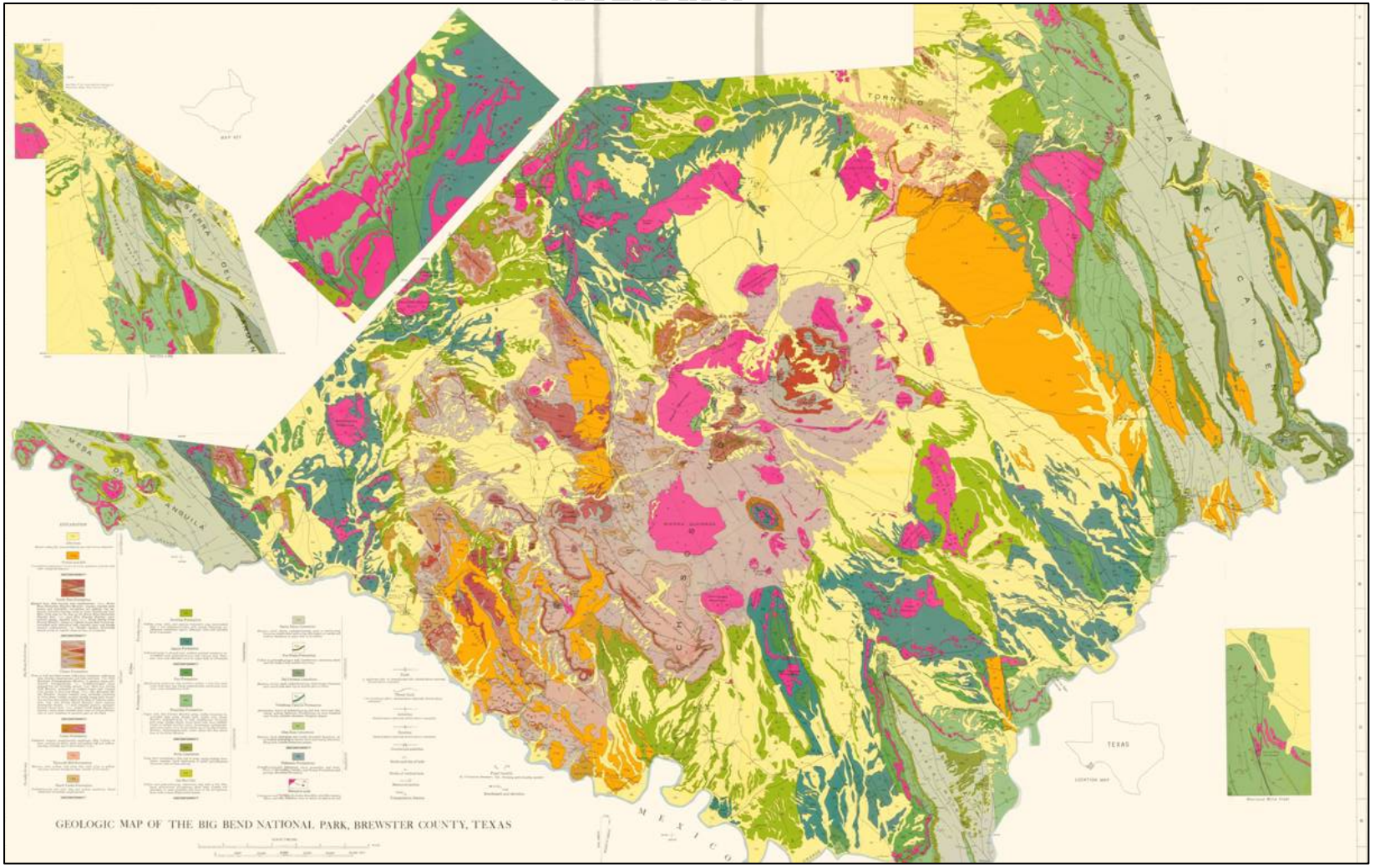

Fig. 26. Geologic map of Big Bend National Park, Brewster County, Texas (Maxwell, 1966).

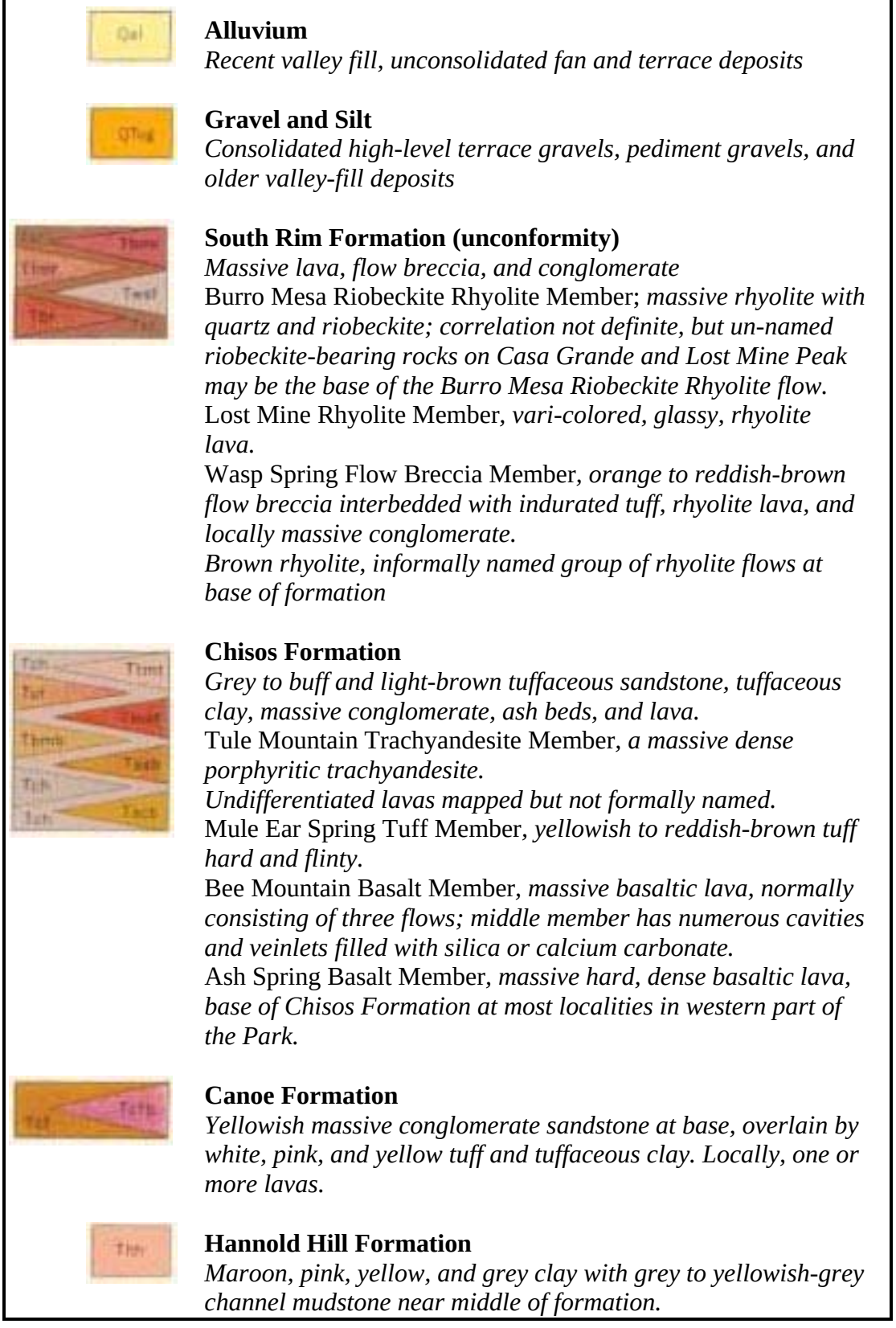

Alluvium
Recent valley fill, unconsolidated fan and terrace deposits

Gravel and Silt
Consolidated high-level terrace gravels, pediment gravels, and older valley-fill deposits

South Rim Formation (unconformity)
Massive lava, flow breccia, and conglomerate
Burro Mesa Riobeckite Rhyolite Member; *massive rhyolite with quartz and riobeckite; correlation not definite, but un-named riobeckite-bearing rocks on Casa Grande and Lost Mine Peak may be the base of the Burro Mesa Riobeckite Rhyolite flow.*
Lost Mine Rhyolite Member, *vari-colored, glassy, rhyolite lava.*
Wasp Spring Flow Breccia Member, *orange to reddish-brown flow breccia interbedded with indurated tuff, rhyolite lava, and locally massive conglomerate.*
Brown rhyolite, informally named group of rhyolite flows at base of formation

Chisos Formation
Grey to buff and light-brown tuffaceous sandstone, tuffaceous clay, massive conglomerate, ash beds, and lava.
Tule Mountain Trachyandesite Member, *a massive dense porphyritic trachyandesite.*
Undifferentiated lavas mapped but not formally named.
Mule Ear Spring Tuff Member, *yellowish to reddish-brown tuff hard and flinty.*
Bee Mountain Basalt Member, *massive basaltic lava, normally consisting of three flows; middle member has numerous cavities and veinlets filled with silica or calcium carbonate.*
Ash Spring Basalt Member, *massive hard, dense basaltic lava, base of Chisos Formation at most localities in western part of the Park.*

Canoe Formation
Yellowish massive conglomerate sandstone at base, overlain by white, pink, and yellow tuff and tuffaceous clay. Locally, one or more lavas.

Hannold Hill Formation
Maroon, pink, yellow, and grey clay with grey to yellowish-grey channel mudstone near middle of formation.

Fig. 27. BBNP geologic map legend. Enlarged and adapted from Maxwell (1966).

Fig. 27, Continued.

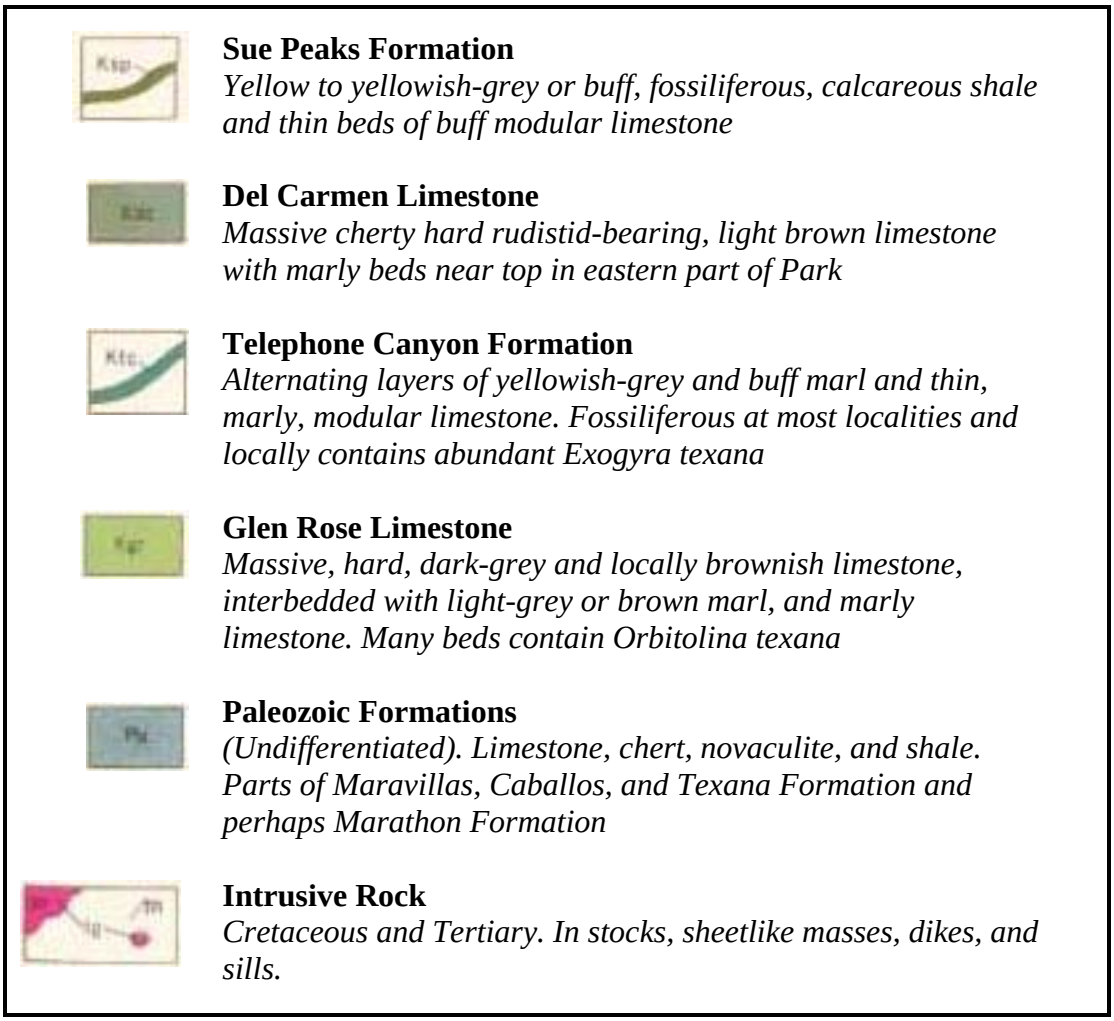

Sue Peaks Formation
Yellow to yellowish-grey or buff, fossiliferous, calcareous shale and thin beds of buff modular limestone

Del Carmen Limestone
Massive cherty hard rudistid-bearing, light brown limestone with marly beds near top in eastern part of Park

Telephone Canyon Formation
Alternating layers of yellowish-grey and buff marl and thin, marly, modular limestone. Fossiliferous at most localities and locally contains abundant Exogyra texana

Glen Rose Limestone
Massive, hard, dark-grey and locally brownish limestone, interbedded with light-grey or brown marl, and marly limestone. Many beds contain Orbitolina texana

Paleozoic Formations
(Undifferentiated). Limestone, chert, novaculite, and shale. Parts of Maravillas, Caballos, and Texana Formation and perhaps Marathon Formation

Intrusive Rock
Cretaceous and Tertiary. In stocks, sheetlike masses, dikes, and sills.

Fig. 27, Continued.

APPENDIX B

Photographs of desert pavement sample sites from Study Area 1 off Old Maverick Road, Study Area 2 off Ross Maxwell Scenic Drive, and Study Area 3 off Croton Springs Road. Black and white meter stick shows a 1 m field of view. GPS locations are noted on the photographs.

Fig. 28. Desert pavement sample sites. Continued on next 7 pages.

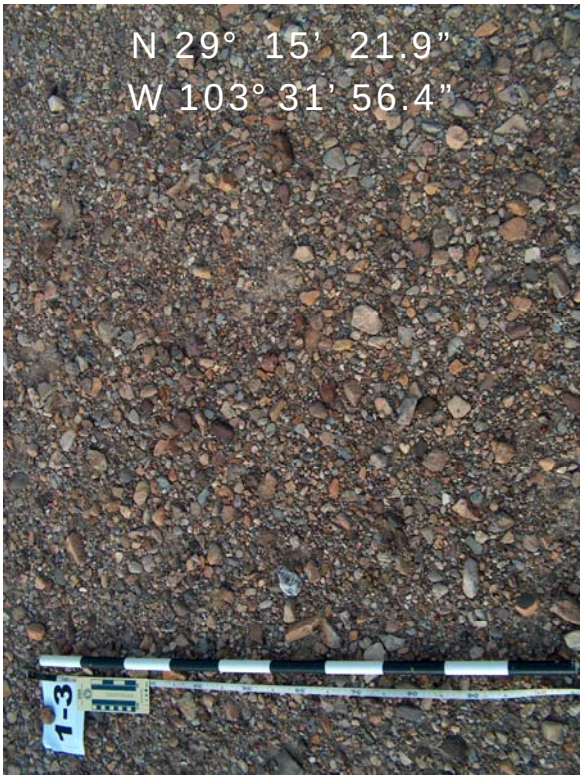
N 29° 15’ 21.9”
W 103° 31’ 56.4”
1-3

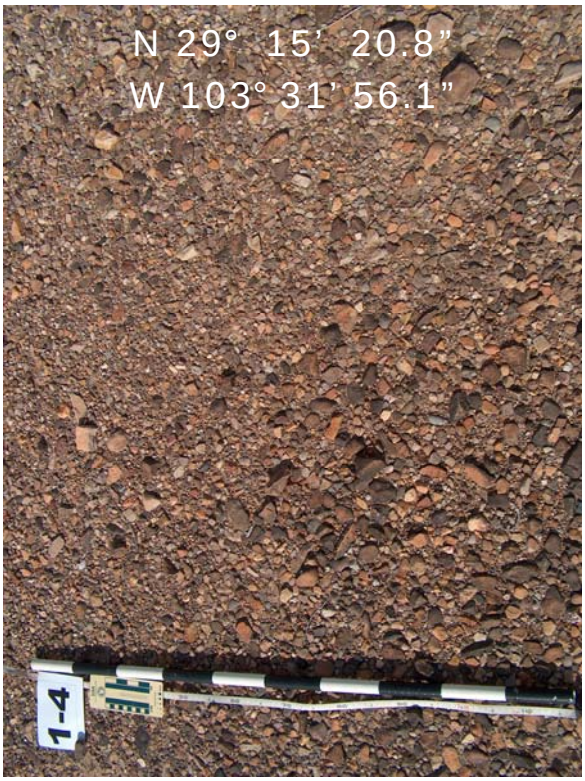
N 29° 15’ 20.8”
W 103° 31’ 56.1”
1-4


N 29° 15’ 21.3”
W 103° 31’ 55.9”
1-5

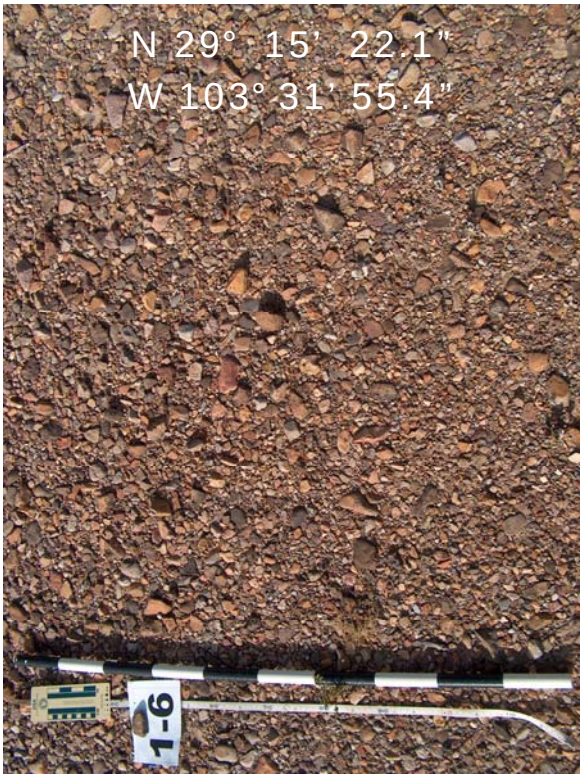
N 29° 15’ 22.1”
W 103° 31’ 55.4”
1-6

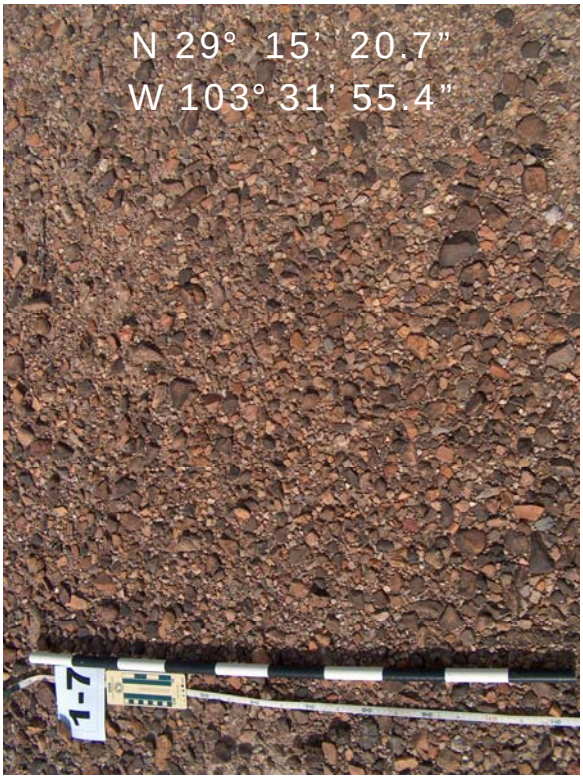
N 29° 15’ 20.7”
W 103° 31’ 55.4”
1-7


N 29° 15’ 21.2”
W 103° 31’ 55.3”
1-8

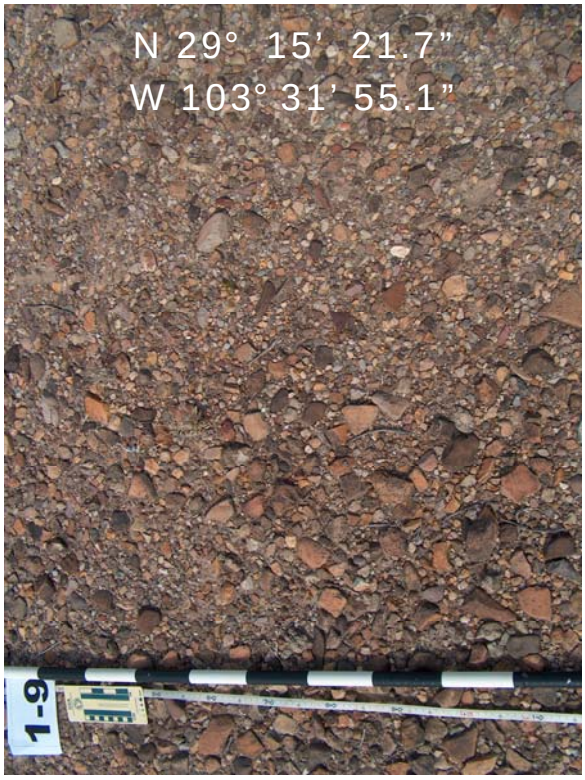
N 29° 15’ 21.7”
W 103° 31’ 55.1”
1-9

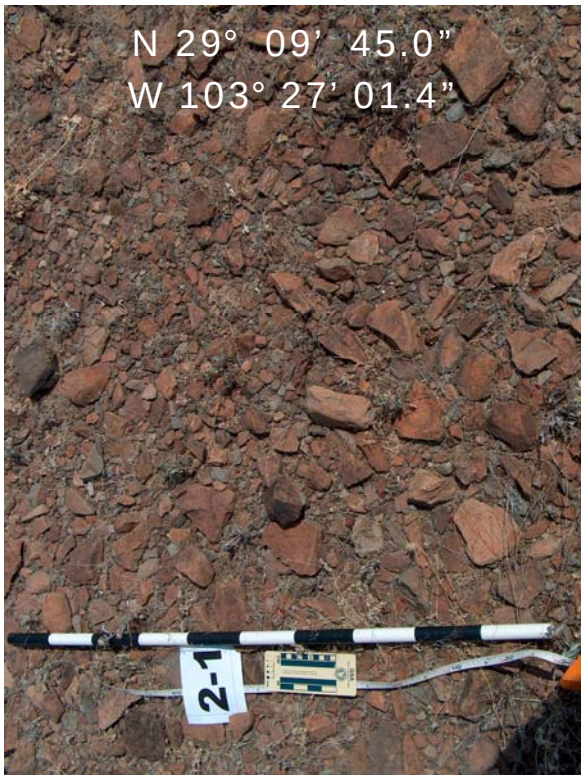
N 29° 09’ 45.0”
W 103° 27’ 01.4”
2-1

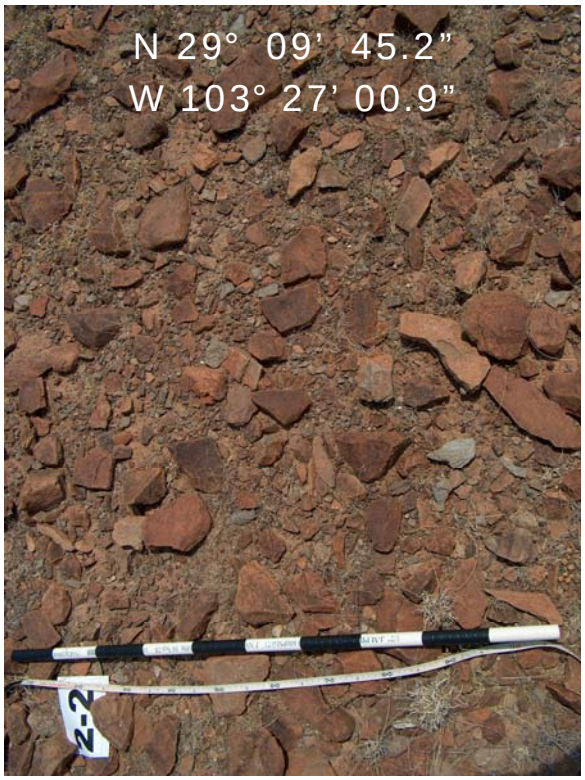
N 29° 09’ 45.2”
W 103° 27’ 00.9”
2-2


N 29° 09’ 45.5”
W 103° 27’ 00.5”
2-3

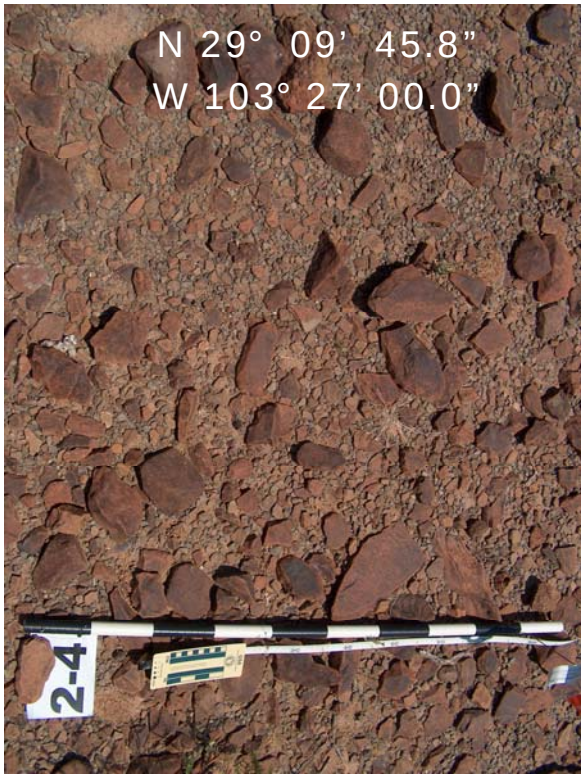
N 29° 09’ 45.8”
W 103° 27’ 00.0”
2-4

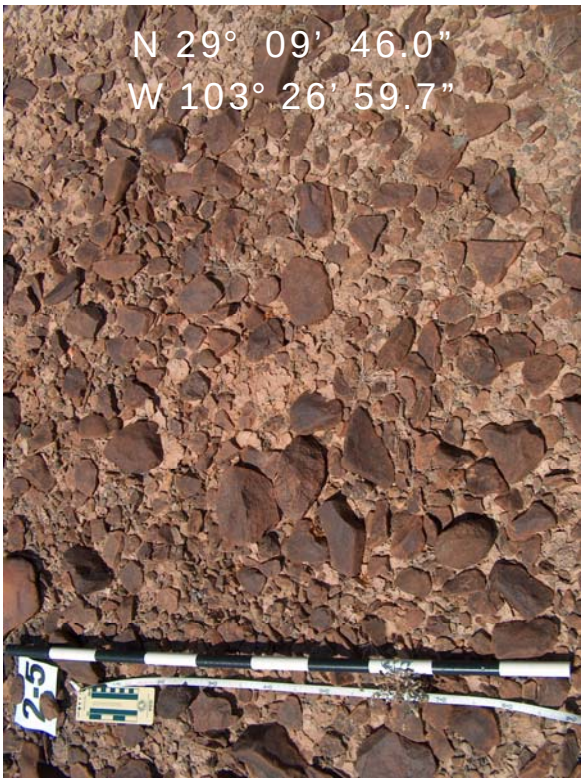
N 29° 09’ 46.0”
W 103° 26’ 59.7”
2-5

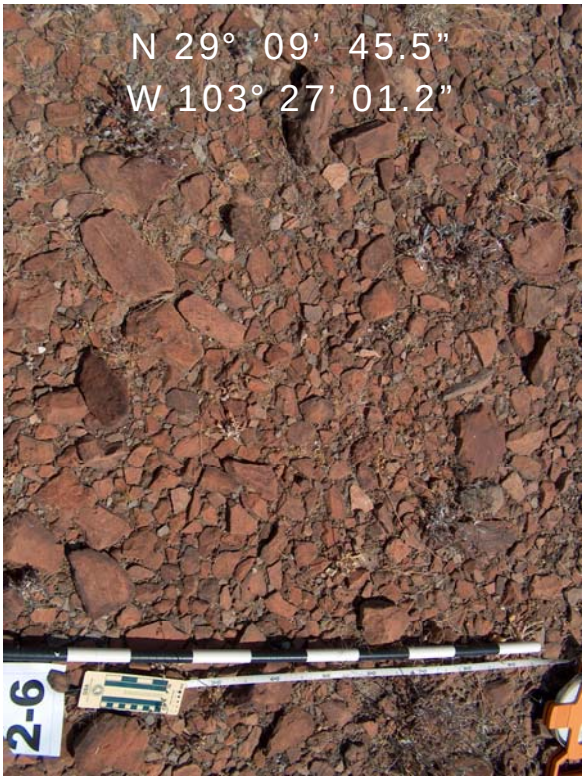
N 29° 09’ 45.5”
W 103° 27’ 01.2”
2-6

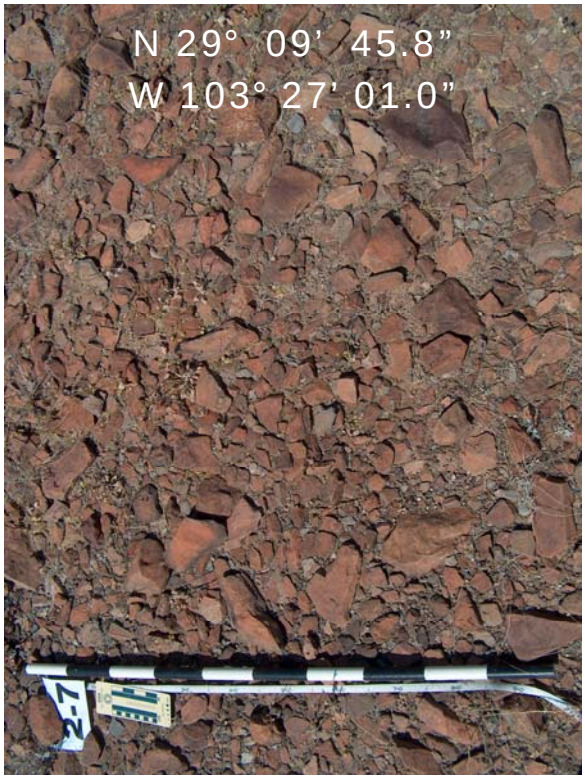
N 29° 09’ 45.8”
W 103° 27’ 01.0”
2-7

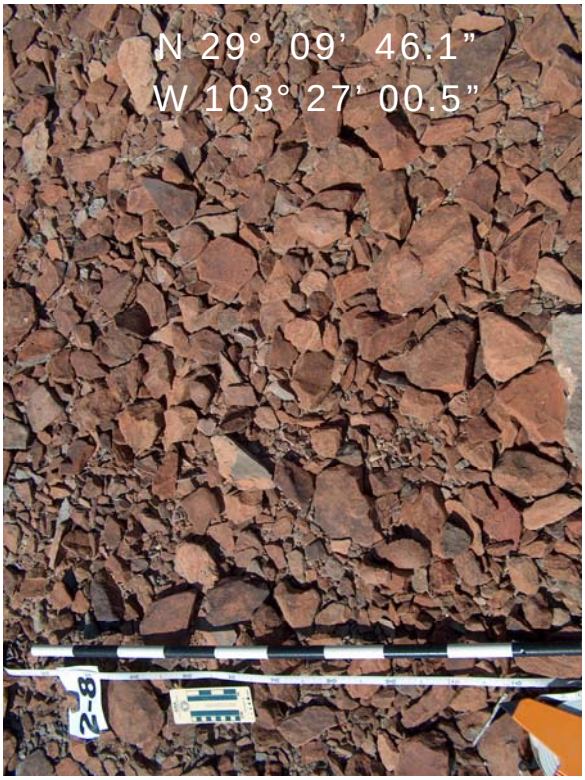
N 29° 09’ 46.1”
W 103° 27’ 00.5”
2-8


N 29° 09’ 46.4”
W 103° 27’ 00.1”
2-9

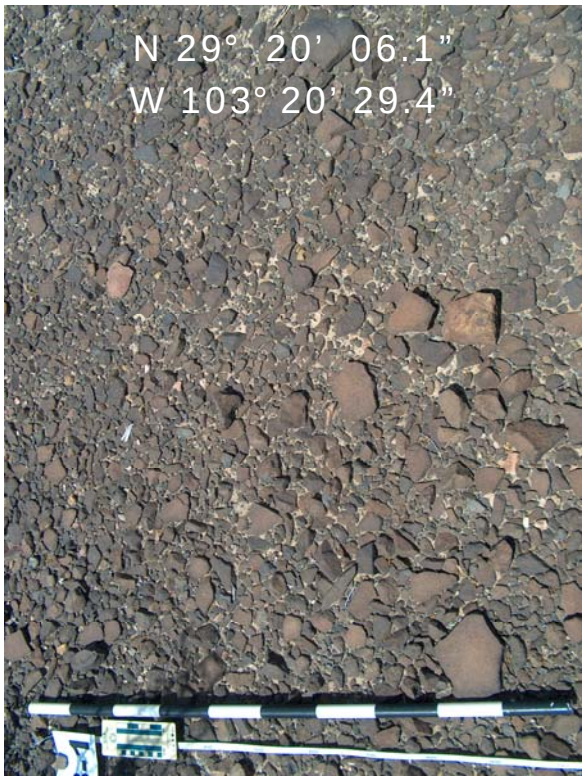
N 29° 20’ 06.1”
W 103° 20’ 29.4”

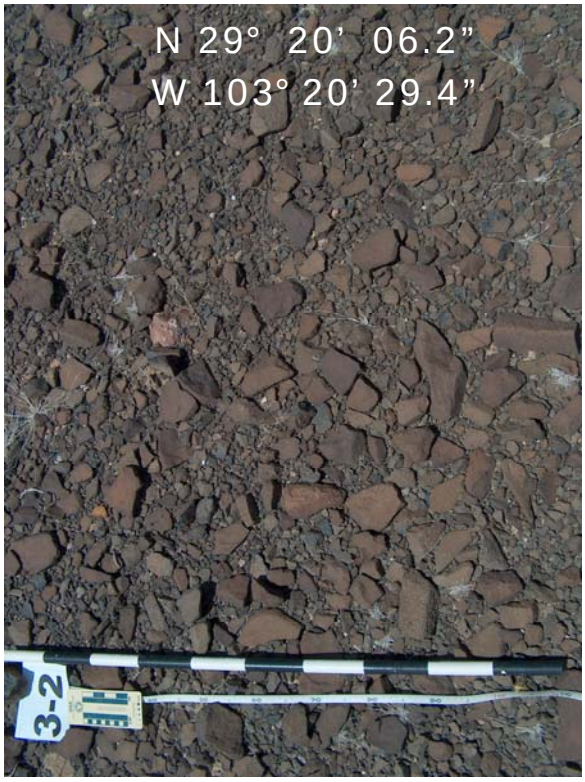
N 29° 20’ 06.2”
W 103° 20’ 29.4”
3-2

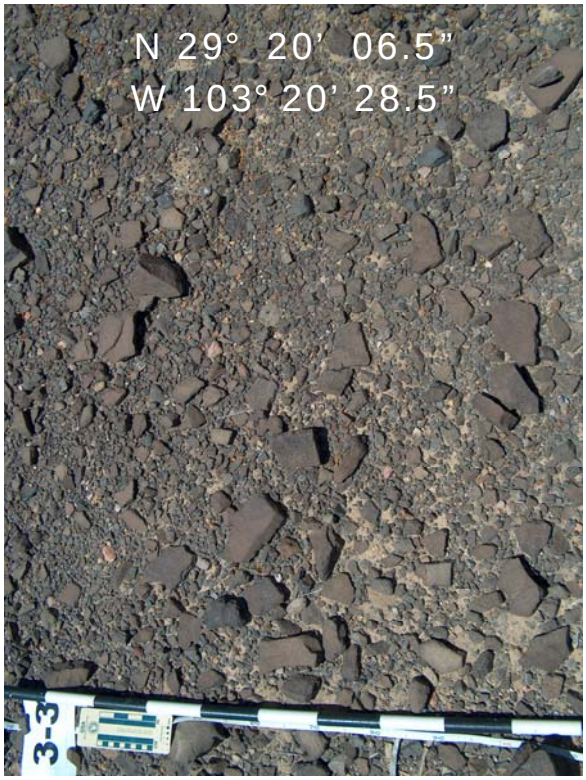
N 29° 20’ 06.5”
W 103° 20’ 28.5”
3-3

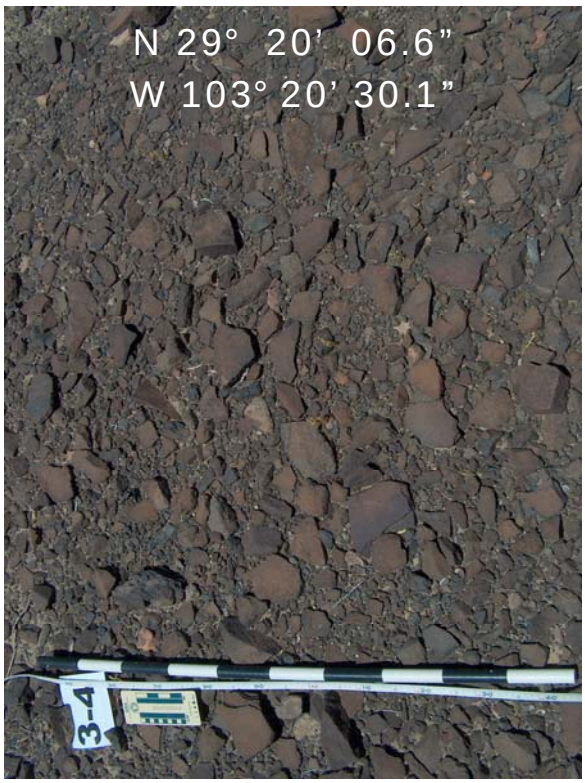
N 29° 20’ 06.6”
W 103° 20’ 30.1”
3-4

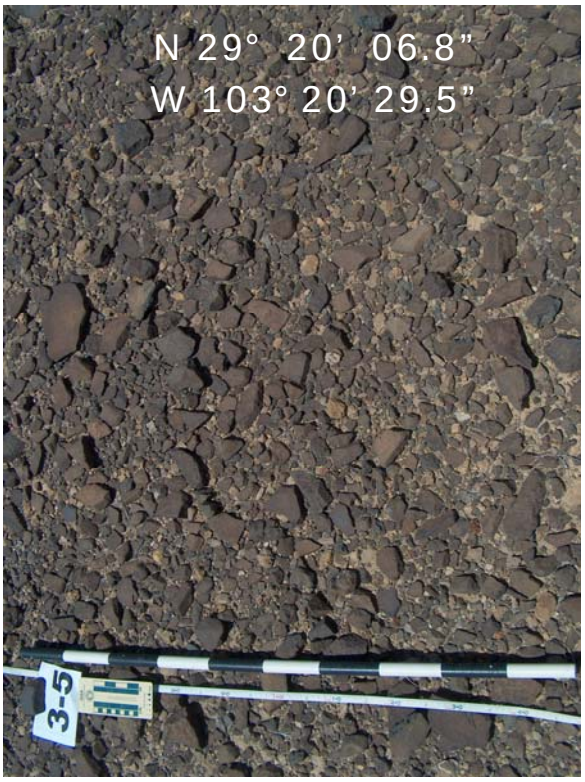
N 29° 20’ 06.8”
W 103° 20’ 29.5”
3-5

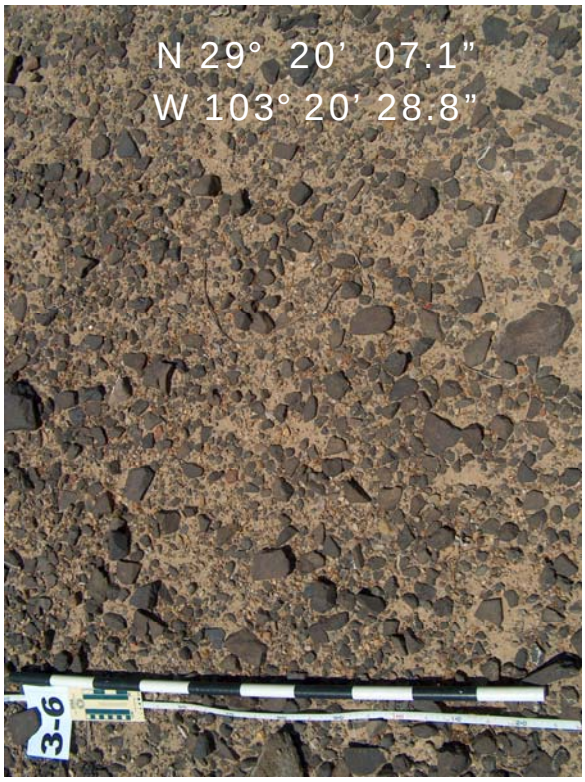
N 29° 20’ 07.1”
W 103° 20’ 28.8”
3-6


N 29° 20’ 07.0”
W 103° 20’ 30.1”
3-7

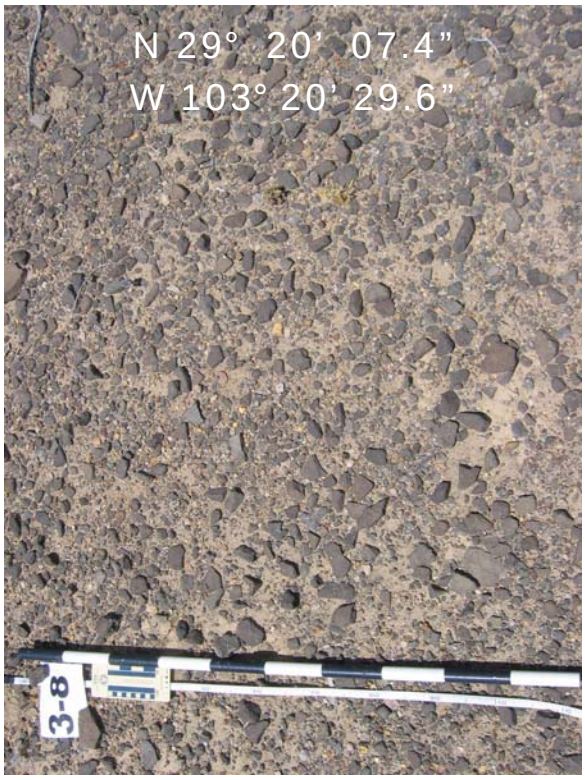
N 29° 20’ 07.4”
W 103° 20’ 29.6”
3-8


N 29° 20’ 07.5”
W 103° 20’ 29.1”
3-6

APPENDIX C

Table 7. Sediment analysis data from surface and subsurface samples

Sample site	Very coarse sand %	Coarse sand %	Medium sand %	Fine sand %	Very fine sand %	Coarse silt %	Fine silt %	Clay %
Sediment samples taken at 2cm below desert pavement surface								
1-1	8.4	5.2	7.7	16.4	18.0	16.7	18.2	9.4
1-2	5.6	5.3	8.9	19.5	20.0	14.8	16.9	9.0
1-3	5.8	4.6	8.2	19.4	19.9	14.9	17.4	9.7
1-4	4.8	3.7	7.1	18.0	18.2	14.5	21.8	11.9
1-5	3.1	3.1	7.2	19.0	18.5	15.7	23.5	9.9
1-6	7.4	5.5	8.4	19.0	20.0	12.6	15.6	11.5
1-7	2.6	2.4	4.8	14.2	16.1	14.3	30.1	15.5
1-8	4.5	3.6	6.9	17.4	17.3	12.9	22.1	15.2
1-9	3.4	4.3	8.1	18.1	17.0	12.7	21.7	14.7
2-1	8.3	7.8	11.0	16.7	17.2	12.5	12.8	13.7
2-2	10.2	8.9	10.3	13.4	14.1	11.2	12.2	19.7
2-3	4.3	3.8	5.6	10.0	14.3	12.0	19.8	30.2
2-4	10.3	5.8	8.3	14.7	13.4	8.9	16.9	21.6
2-5	4.8	3.0	3.9	8.7	11.8	11.7	21.1	35.0
2-6	5.7	5.9	8.7	15.2	17.5	12.5	17.7	16.7
2-7	8.1	7.5	7.9	13.3	17.2	13.4	17.1	15.4
2-8	2.2	2.3	3.6	7.3	12.2	16.0	25.9	30.4
2-9	3.4	4.2	6.9	15.6	17.3	12.9	18.1	21.6
3-1	3.3	1.8	3.0	28.8	22.2	10.7	14.4	15.8
3-2	7.7	2.5	2.3	23.1	18.0	7.9	11.2	27.3
3-3	5.1	2.3	3.7	30.7	19.6	7.5	10.6	20.5
3-4	5.9	2.8	2.8	21.1	15.1	7.7	16.6	28.0
3-5	5.6	2.8	4.1	27.9	21.6	9.6	13.4	15.0
3-6	2.6	2.2	3.9	32.6	22.7	8.9	11.3	15.8
3-7	6.3	2.4	2.3	23.5	16.9	6.6	13.2	28.7
3-8	4.6	2.9	5.9	38.9	14.8	4.8	9.5	18.5
3-9	2.2	2.3	3.2	28.2	26.8	8.2	12.0	17.1
Sediment samples taken at 10 cm below desert pavement surface								
1	8.1	7.0	7.8	15.8	15.2	12.1	18.2	15.7
2	*destroyed during lab analysis*			*N/A*	*N/A*	*N/A*	*N/A*	*N/A*
3	1.7	1.3	1.9	17.5	12.2	12.3	15.1	38.0

VITA

Name:	Courtney Michelle Harmon
Address:	Texas A&M University, Department of Geography 810 O&M Building, TAMU Mail Stop 3147 College Station, Texas 77843-3147
Email Address:	Harmon03@neo.tamu.edu
Education:	B.S., Earth Sciences, Texas A&M University, 2003 M.S., Geography, Texas A&M University, 2006